



**HAL**  
open science

# Wave Climate Projections off Coastal French Guiana based on High-Resolution Modelling over the Atlantic Ocean

Maurizio d'Anna, Léopold Védie, Ali Belmadani, Déborah Idier, Rémi Thiéblemont, Philippe Palany, François Longueville

► **To cite this version:**

Maurizio d'Anna, Léopold Védie, Ali Belmadani, Déborah Idier, Rémi Thiéblemont, et al.. Wave Climate Projections off Coastal French Guiana based on High-Resolution Modelling over the Atlantic Ocean. *Ocean Modelling*, 2024, 10.1016/j.ocemod.2024.102468 . hal-04813791v1

**HAL Id: hal-04813791**

**<https://brgm.hal.science/hal-04813791v1>**

Submitted on 2 Dec 2024 (v1), last revised 6 Jan 2025 (v2)

**HAL** is a multi-disciplinary open access archive for the deposit and dissemination of scientific research documents, whether they are published or not. The documents may come from teaching and research institutions in France or abroad, or from public or private research centers.

L'archive ouverte pluridisciplinaire **HAL**, est destinée au dépôt et à la diffusion de documents scientifiques de niveau recherche, publiés ou non, émanant des établissements d'enseignement et de recherche français ou étrangers, des laboratoires publics ou privés.



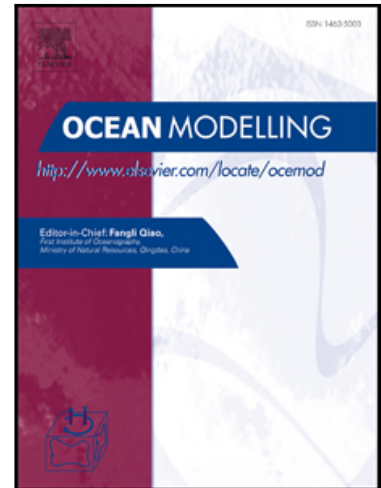
Distributed under a Creative Commons Attribution 4.0 International License

## Journal Pre-proof

Wave Climate Projections off Coastal French Guiana based on High-Resolution Modelling over the Atlantic Ocean

Maurizio D'Anna , Léopold Védie , Ali Belmadani , Déborah Idier , Remi Thiéblemont , Philippe Palany , François Longueville

PII: S1463-5003(24)00154-9  
DOI: <https://doi.org/10.1016/j.ocemod.2024.102468>  
Reference: OCEMOD 102468



To appear in: *Ocean Modelling*

Received date: 2 August 2024  
Revised date: 3 November 2024  
Accepted date: 19 November 2024

Please cite this article as: Maurizio D'Anna , Léopold Védie , Ali Belmadani , Déborah Idier , Remi Thiéblemont , Philippe Palany , François Longueville , Wave Climate Projections off Coastal French Guiana based on High-Resolution Modelling over the Atlantic Ocean, *Ocean Modelling* (2024), doi: <https://doi.org/10.1016/j.ocemod.2024.102468>

This is a PDF file of an article that has undergone enhancements after acceptance, such as the addition of a cover page and metadata, and formatting for readability, but it is not yet the definitive version of record. This version will undergo additional copyediting, typesetting and review before it is published in its final form, but we are providing this version to give early visibility of the article. Please note that, during the production process, errors may be discovered which could affect the content, and all legal disclaimers that apply to the journal pertain.

© 2024 Published by Elsevier Ltd.

## Highlights

- Basin-scale wave model forced with high-resolution atmospheric global climate model
- Future winter-wave climate projections offshore of French Guiana
- Decrease in winter mean wave height, period, and clockwise rotation of direction

Journal Pre-proof

# Wave Climate Projections off Coastal French Guiana based on High-Resolution Modelling over the Atlantic Ocean

Maurizio D'Anna\*<sup>1</sup>, Léopold Vedie<sup>2</sup>, Ali Belmadani<sup>3,4</sup>, Déborah Idier<sup>5</sup>, Remi Thiéblemont<sup>5</sup>, Philippe Palany<sup>2</sup>, and François Longueville<sup>1</sup>

<sup>1</sup>BRGM, 25 Av. Leonard de Vinci, 33600, Pessac, France.

<sup>2</sup>Météo-France, Direction Interrégionale Antilles-Guyane, Fort-de-France, Martinique, France

<sup>3</sup>Météo-France, École Nationale de la Météorologie, Toulouse, France

<sup>4</sup>CNRM, Université de Toulouse, Météo-France, CNRS, Toulouse, France

<sup>5</sup>BRGM, 3 Av. Guillemin, 45060, Orléans, France.

\*Corresponding Author

## Abstract

Global warming is altering the atmosphere and ocean dynamics worldwide, including patterns in the generation and propagation of ocean waves, which are important drivers of coastal evolution, flood risk, and renewable energy. In French Guiana (northern South America), where most of the population is concentrated in coastal areas, understanding future wave climate change is critical for regional development, planning and adaptation purposes. The most energetic waves typically occur in boreal winter, in the form of long-distance swell originating from the mid-latitude North Atlantic Ocean. However, existing high-resolution wave climate projections that cover the French Guiana region focus on the hurricane season only (summer-fall). In this study, we used a state-of-the-art basin-scale spectral wave model and wind fields from a high-resolution atmospheric global climate model to simulate present and future winter (November to April) wave climate offshore of French Guiana. The model performance was evaluated against wave data from ERA5 reanalysis, satellite altimetry and coastal buoys between 1984 and 2013. For the future greenhouse gas emission scenario (Representative Concentration Pathway) RCP-8.5, we found a statistically significant overall projected decrease (~5%) in wintertime average significant wave height and mean wave period, with a ~1° clockwise rotation of mean wave direction. The results suggest that these decreasing trends are primarily driven by changes in large-scale patterns across the Atlantic that counteract an expected increase in local wind speed. We discuss the implications of such projections for mud-bank dynamics along coastal French Guiana, although further local studies are required to address future coastal evolution and hazards. Finally, we identify a need for more *in situ* wave data near French Guiana to improve quantitative assessments of model performance and allow a correction of possible model biases.

**Keywords:** Climate change; Wave projections; Atlantic Ocean; French Guiana.

# 1 Introduction

Climate change is altering the atmospheric circulation patterns that drive the generation and propagation of ocean waves (Reguero et al., 2019), and is expected to reshape global wave climate and associated extremes throughout the 21<sup>st</sup> century (Casas-Prat et al., 2024; Hemer et al., 2013a; Lemos et al., 2021). Together with other hydrodynamic features, surface waves contribute to numerous coastal processes such as sediment transport, run-up and flooding (Toimil et al., 2020). Therefore, understanding the future evolution of wave climate is a key step for coastal management in the frame of climate adaptation (Cooley et al., 2022).

Located in the northern South America/equatorial Atlantic region, French Guiana hosts one of the most unique coastal systems on Earth. Embedded in the 1500-km long stretch of coast extending between the Amazon and Orinoco river mouths, it features dynamic mud banks formed by the Amazon River sediment discharge (Froidefond et al., 1988). These mud banks continuously interact with sandy beaches and rocky outcrops (Anthony et al., 2010; Jolivet et al., 2022), causing dynamic morphological and ecological changes on monthly to decadal time scales (Gensac et al., 2011; Wells & Kemp, 1986). Observations of the local shoreline evolution indicated that most of the erosion occurs during the rain season (April-June) in response to northern swells and spring tide (Aertgeerts & Longueville, 2018; Longueville, 2017; Longueville & Lanson, 2022). Besides, the French Guiana coastal zone gathers ~90% of the local population, as well as important assets such as the European Spatial Agency spaceport in Kourou, raising concerns about the exposure of the region to coastal hazards.

The complex morphodynamics of this coast is dominated by the alongshore migration of mud banks (Gardel & Gratiot, 2005), which is primarily controlled by ocean waves and currents (Gratiot et al., 2007). While recent studies have made significant progress in unravelling the inherent link between mud bank migration and incident waves (Abascal-Zorrilla et al., 2018, 2020; Gensac et al., 2015; Jolivet et al., 2019; Vantrepotte et al., 2013), future regional wave projections are essential in order to identify potential variations in the regime of mud bank dynamics and the cascading implications. As the local wave climate is strongly influenced by incoming swells from the North Atlantic Ocean, especially during the winter season (Anthony et al., 2011; Vantrepotte et al., 2013; Young, 1999), future wave projections offshore of French Guiana need to account for the effect of climate change over the entire Atlantic basin.

Over the last decade, much effort has been dedicated to projections of changes in mean and extreme wave conditions across the 21<sup>st</sup> century, on global scale (Camus et al., 2017; Casas-Prat et al., 2018; Fan et al., 2013, 2014; Hemer et al., 2013a; Hemer et al., 2013b; Lemos et al., 2019; Lobeto et al., 2021, 2022; Meucci et al., 2020, 2024; Mori et al., 2010, 2013; Semedo et al., 2012, 2013, 2018; Wang et al., 2014) and Atlantic basin scale (Belmadani et al., 2021; Bernardino et al., 2021; Cantet et al., 2021; D'Agostini et al., 2022; Webb et al., 2018). Many individual studies contributed to the

Coordinated Ocean Wave Climate Project (COWCLIP, Hemer et al., 2018), forming a multi-model ensemble of global wave projections (Morim et al., 2020) forced by different Global Climate Models (GCMs) from the CMIP5 (Coupled Model Intercomparison Project, phase 5). This ensemble allowed mapping the spatially variable robustness (statistical significance) of the projected wave changes while analysing the uncertainties related to the use of different GCMs, wave models/statistical approaches and future greenhouse gas emission scenarios (Morim et al. 2019; Yadav et al. 2024). While most studies showed a consensus in modelled future trends over a large fraction of the Atlantic, the typical resolutions of GCMs (1-2°) and wave models (~1°) (Morim et al., 2020) result in hardly robust (not statistically significant) projections in tropical regions (Morim et al. 2019; Yadav et al. 2024). In the latter areas, modelling summertime tropical cyclones and the related waves requires finer resolutions of the forcing wind fields (Timmermans et al., 2017). However, during wintertime (DJF), when tropical cyclones are not expected, the COWCLIP ensemble shows yet a lack of robustness and large uncertainties (i.e., ensemble spread) (Morim et al., 2019). In the French Guiana area, the COWCLIP ensemble shows statistically significant change only in mean wave direction, and only at the north of the French territory's coastal area (Morim et al., 2019). Therefore, the COWCLIP projections in French Guiana as well as most of the tropical Atlantic region remain inconclusive, and more high-resolution studies are required to achieve robust wave projections in these areas.

Lately, updated GCMs with higher resolutions and improved physics have been developed within the more recent CMIP6 (Eyring et al., 2016), opening the way for a new generation of global wave projections (Meucci et al., 2024). Yet, these projections rely on ~1° resolution GCMs forcing wave models on a ~1° grid, and keep showing significant limitations in representing tropical wave climates (Meucci et al., 2023, 2024). Therefore, future trends in wave climate and extremes in the French Guiana region are still unclear.

Recently, Belmadani et al. (2021) derived future wave projections over the North Atlantic basin for the summer-fall (hurricane) season, focusing on changes in tropical cyclones and related wave extremes. They used wind fields from a global atmospheric GCM with a zoomed 0.15-0.25° grid over the North Atlantic to force a wave model covering the whole Atlantic basin at 0.5° resolution and including a nested 0.1° grid over the tropical North Atlantic band. Such fine resolutions allowed accounting for the influence of tropical cyclones on future wave climate, and producing statistically significant projections over most of the Atlantic basin. However, projections driven by high-resolution wind fields are still missing for the winter season, when French Guiana hydro- and morpho-dynamic coastal processes are most influenced by wave climate (Gratiot et al., 2007). In addition, while occurring typically during summer and fall, Atlantic tropical cyclones can also originate during the winter season (Collins & Roache, 2017), reinforcing the need for resolving wind fields at fine resolution. The current study aims at addressing future changes in mean and extreme wave conditions offshore of French Guiana for the winter season based on high-resolution wind

fields, in order to inform future assessments of climate change impact on the local coastal processes. The current results will also complement existing summer season projections, advancing the state of the art of wave projections over the Atlantic Ocean. For this purpose, we use the high-resolution GCM winds (0.15-0.25°) and wave model (0.5°) adopted by Belmadani et al. (2021) over the Atlantic basin. The simulations are forced with a single GCM and consider a single scenario of future greenhouse gas emissions (Representative Concentration Pathway) RCP-8.5. We produced 5-member ensembles of multidecadal historical and future winter wave conditions over the Atlantic Ocean. The wave model performance offshore of French Guiana is evaluated against the ERA5 reanalysis, satellite altimetry and available coastal wave buoy data. We discuss the complementarity of the wave projections presented here with existing studies focused on the summer-fall season (Belmadani et al., 2021), leading to year-round state-of-the-art wave climate projections over the Atlantic Ocean, with particular focus on French Guiana. Finally, we discuss the annual and monthly COWCLIP multi-model projections near French Guiana to provide additional insights on future wave climate change in this area. While a full uncertainty assessment is hindered by the computational cost of such large-scale models, the current wave projections can provide a valuable contribution to future generations of high-resolution multi-model ensembles.

The remainder of the paper includes a description of the wind and wave data, the wave model and the methodology used herein (Section 2). The results of the model performance assessment and the wave projections are illustrated in Section 3 and discussed in Section 4. The conclusions of this work are drawn in Section 5.

## 2 Material and method

### 2.1 Wind data

Modelling the generation of ocean waves requires information on wind speed and direction near the sea surface. We used wind fields produced by Chauvin et al. (2020) who applied the very-high-resolution ARPEGE-Climat model, which is the atmospheric component of the CNRM-CM coupled GCM developed at Météo France.

Chauvin et al. run ARPEGE-Climat in the configuration adopted for CNRM-CM6 within the latest CMIP6 (Roehrig et al., 2020; Voldoire et al., 2019), but with a rotated and stretched spatial grid of 14km – 30km resolution over the tropical Atlantic region (Cantet et al., 2021). These settings allow the resolution of small-scale atmospheric patterns such as tropical cyclones (Chauvin et al., 2020), and small-scale details of the broader North Atlantic extratropical storms, ensuring that associated swells that may reach the coast of French Guiana are not overlooked.

ARPEGE-Climat was forced with monthly sea surface temperature (SST) fields obtained from the CMIP5 CNRM-CM5 model (Voldoire et al., 2013), for the historical period (1965-2013, hereon Hist-Model) and future (2031-2080) RCP-8.5 scenario. These prescribed SST fields were previously

corrected using observed monthly SSTs (HadISST1, Rayner, 2003). Chauvin et al. (2020) also forced ARPEGE-Climat using the observed HadISST1 SSTs directly, from 1965 to 2014, in an additional experiment (hereon Hist-Obs) for model comparison with observation data (Table 1).

Each experiment (Hist-Obs, Hist-Model and RCP-8.5) includes an ensemble of five model realizations (members) based on different initial conditions, i.e. forced with the same SST fields but exhibiting different chronologies of meteorological events. For instance, in the Hist-Obs experiment the five members were run with the same series of SSTs but with initial conditions (1<sup>st</sup> of January) corresponding to HadISST1 observations on the 1<sup>st</sup> of January of different years. For each experiment and respective ensemble members, ARPEGE-Climat simulations provide 6-hourly fields of 10-m wind vectors interpolated over a 0.5° regular grid.

The reader is referred to Chauvin et al., (2020) for further details on the climate model and the associated simulations. For our applications, we extracted wind data from the latest modelled 29 winter seasons (November – April) for each experiment and ensemble member proposed by Chauvin et al., (2020), i.e. Hist-Obs, Hist-Model and RCP-8.5 (Table 1).

**Table 1.** Summary of ARPEGE-Climat simulations including: SST forcing and experiments; time slices modelled by Chauvin et al. (2020) and used in the present study; number of model realizations.

ARPEGE-Climat model experiment	Forcing monthly SST	Simulated time slice	Extracted data	# ensemble members
Hist-Obs	HadISST1	1965-2014	November 1985-April 1986 to November 2013-April 2014 (hereafter 1985-2013)	5
Hist-Model	CNRM-CM5, historical, corrected with HadISST1	1965-2013	November 1984-April 1985 to November 2012-April 2013 (hereafter 1984-2012)	5
RCP-8.5	CNRM-CM5, RCP8.5, corrected with HadISST1	2031-2080	November 2051-April 2052 to November 2079-April 2080 (hereafter 2051-2079)	5

Over the historical period, the ARPEGE-Climat wintertime (NDJFMA) mean wind speed 10 m above the sea surface ( $U_{10}$ ) reaches its largest values in the tropical band (roughly along the 15°N parallel) and decreases towards French Guiana. This pattern represents typical winter conditions, characterized by stronger trade winds and the Intertropical Convergence Zone located closer to the equator (Figure 1a) compared to summer (Figure 3a of Belmadani et al., 2021). In the RCP-8.5 future scenario, ARPEGE-Climat projects a slight intensification of the northeasterly trade winds, with a statistically significant increase in mean  $U_{10}$  near northern South America, including the French Guiana region (Figure 1b). In addition, over the southeastern area offshore of French Guiana,



the wind field undergoes a mild counter-clockwise rotation (Figure S1). In the mid-latitudes (30–50°N) of the Atlantic basin, changes are rather heterogeneous, although the projections show a statistically significant overall reduction of winter mean  $U_{10}$  in this region (Figure 1b). The projected changes and the respective statistical significance are estimated using the method presented in Section 2.4.3.

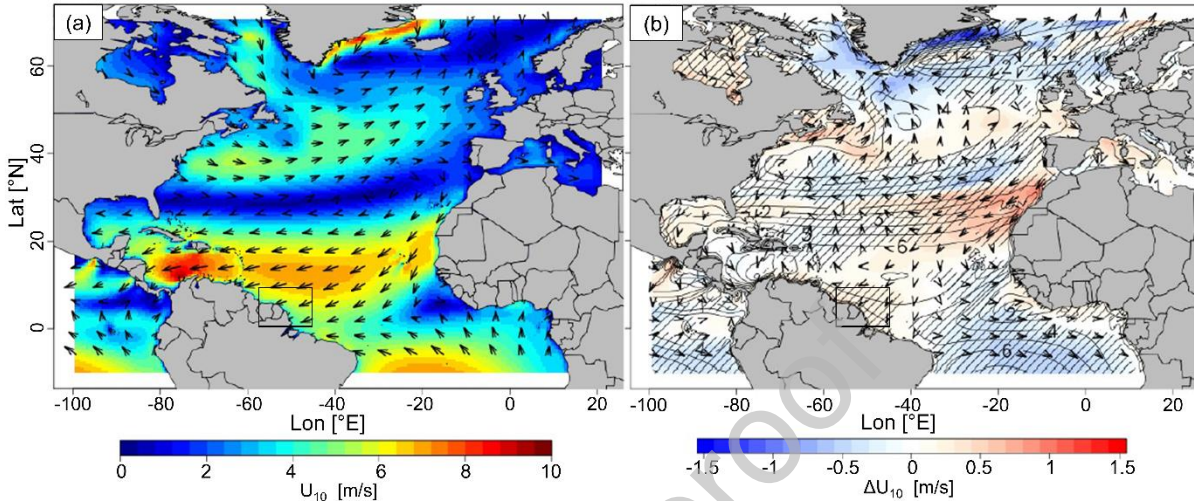


**Figure 1.** Mean present-climate NDJFMA surface wind speed  $U_{10}$  (shading,  $\text{m s}^{-1}$ ) and direction (arrows) for the (a) Hist-Obs (1985-2013) experiment, and respective changes ( $\Delta U_{10}$  shading,  $\text{m s}^{-1}$  and directional arrows) for the (b) future RCP-8.5 (2051-2080) scenario. Hatchings indicate statistically significant changes based on Student's t-test and FDR control (see Section 2.4.3). Black boxes indicate the region considered for the French Guiana regional analyses (see Section 2.4.1).

## 2.2 Wave data

Data of past offshore wave conditions is fundamental to evaluate the wave model performance, and support the interpretation of wave projections with the associated uncertainties in the French Guiana region. The following sections introduce the available data used for model comparison over the historical period (Hist-Obs).

### 2.2.1 ERA5 reanalysis

ERA5 (Hersbach et al., 2020) is a high-resolution (31 km grid cell size, regridded data available at 0.5° resolution) hourly reanalysis of global atmospheric, land surface and ocean surface variables produced by the European Centre for Medium-Range Weather Forecasts (ECMWF) within the Copernicus Climate Change Services. The reanalysis is based on a rich set of globally distributed data from modelling and observation starting from 1940, and includes the reconstruction of hourly wave conditions obtained from an atmospheric model coupled with the European Centre Wave Action Model (ECWAM). For the model comparison, we extracted ERA5 estimates of significant wave height ( $H_s$ ), mean wave period ( $T_m$ ) and mean wave direction ( $D_m$ ) from 1985 to 2013.

Global estimates of historical wave hindcasts and reanalyses such as ERA5 are affected by uncertainties due to different calibration data and modelling approaches (Erikson et al., 2022; Kodaira et al., 2023; Morim et al., 2022, 2023). In particular, ERA5 has been shown to underestimate wave heights in the North Atlantic region (Dodet et al., 2020; Hawkins et al., 2022; Kodaira et al., 2023; Timmermans et al., 2020) and, like most historical datasets (excluding wave buoys), is not expected to provide accurate estimates in coastal areas, where complex nearshore processes are not resolved by such global models. However, during the winter season, most available datasets show consistent trends over most of the Atlantic Ocean (Erikson et al., 2022). For these reasons, we conducted complementary comparisons of the historical model runs (Hist-Obs) against the observed satellite and coastal wave buoy data (Section 2.2.2).

### 2.2.2 Wave buoys and satellite data

Four wave buoys were deployed in different locations off the coast of French Guiana, with data records available from the *Centre d'Archivage National de Données de Houle In Situ* (CANDHIS). For the comparison with historical wave simulations (Sections 3.1 and 2.4.2), we used two of these buoys located at ~20 km offshore of Cayenne (97304) and Kourou (97303), both at 20 m depth (Figures 2a,b). Data from the two remaining buoys are excluded as they are likely affected by local coastal processes (Text S1 of Supplementary Material).

Figures 2c,d show the yearly and monthly distributions of 30-min wave records available from these two buoys during winter. The temporal coverage of the datasets is limited (Figure 2c) to one winter for the 97303 buoy and two winters for the 97304 buoy, with multiple gaps (Figure 2d).

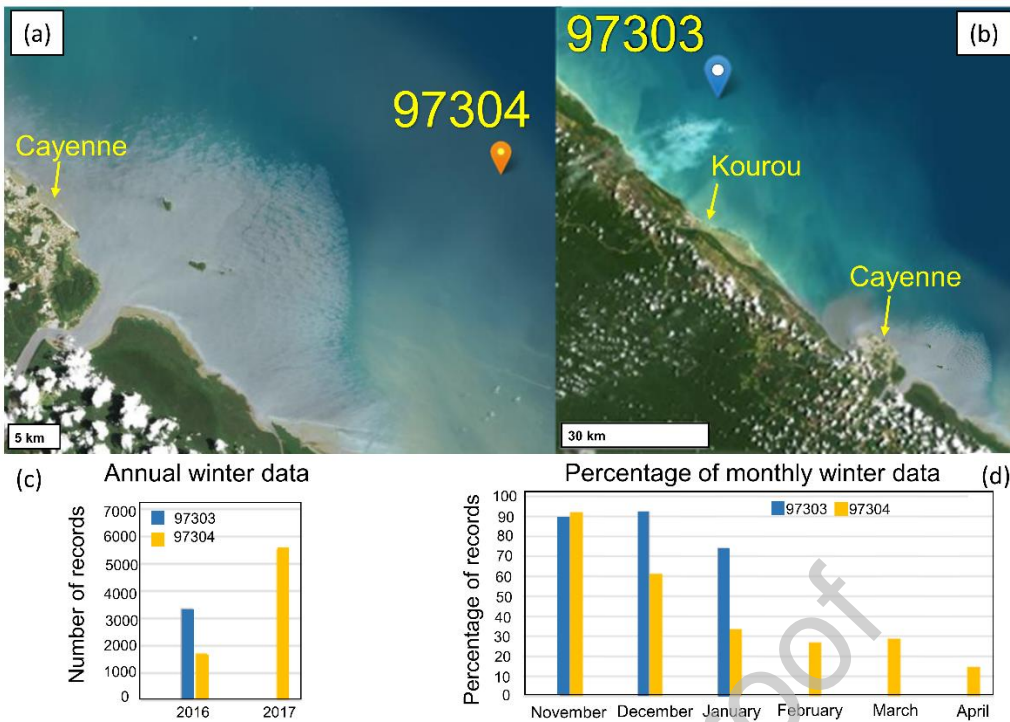


**Figure 2.** Locations of wave buoys in French Guiana's coastal region, offshore of (a) Cayenne (97304) and (a) Kourou (97303) (source: <https://candhis.cerema.fr/public/cartes.php>), and the respective (c) annual number of semi-hourly records during winter (NDJFMA) and (d) monthly percentage of available winter data.

Wave observations off the coasts of French Guiana are also available from satellite altimetry. The European Space Agency Climate Change Initiative (ESA-CCI) level 4 multi-mission product version 1.1 (Dodet et al., 2020; Piollé et al., 2020) provides monthly mean  $H_s$  with a  $1^\circ$  (~110 km) resolution. ESA-CCI data also include monthly exceedance probabilities of  $H_s$  for the 1 m, 1.5 m, 2 m and 3 m threshold values. Along the coastal band, the mean and extreme  $H_s$  estimates should be interpreted carefully, as they may be contaminated by the influence of land and wave form retrievals. We note that satellite data are associated with uncertainties due to e.g. atmospheric corrections and sampling frequency, and are only available from 1991, limiting the comparison with the Hist-Obs results to the 1991-2013 23-year period. While the satellite data cover a shorter period than ERA5, they are derived from observations and are not affected by the limitations of numerical modelling. In addition, a 23-year record remains sufficient for an assessment of model performances. On the other hand, while buoy records provide *in situ* direct information that is not affected by biases associated with modelling (e.g. reanalysis) and processing (e.g. satellite altimetry), they are limited to very localised areas and cover short periods of time. Therefore, the complementary strengths of the three data sources (ERA5, ESA-CCI, CANDHIS) provides more confidence in the interpretation of the model performance over the historical period.

## 2.3 Wave model

We modelled past and future wave conditions offshore of French Guiana using the MFWAM (Météo-France Wave Action Model), an operational third-generation spectral wave model. MFWAM was developed by Météo-France on the basis of WAM (WAMDI-Group, 1988), which is widely used for global and regional modelling studies including future projections that contributed to the COWCLIP ensemble (e.g. Semedo et al., 2018).

The model simulates the generation and propagation of wave energy in response to forcing wind fields by resolving the spectral energy balance, adopting the dissipation term proposed by Ardhuin et al. (2010) and updated by the Copernicus Marine Service. MFWAM also has a similar configuration of ECWAM used to produce ERA5 data. The modelled spectra are discretized into 24 directions ( $15^\circ$  interval) and 30 frequencies ranging from 0.035Hz to 0.58Hz. MFWAM is forced with 2-D 10-m wind time series, produces 3-hourly values of  $H_s$ ,  $T_m$  and  $D_m$ , and has been extensively validated against wave buoy data, showing among the best forecasting skill across the Atlantic Ocean (Bidlot, 2017).

Here, we run MFWAM in the configuration adopted by Belmadani et al., (2021), where the model domain covers most of the North and South Atlantic basins ( $59.5^\circ\text{S}$  to  $70^\circ\text{N}$ ) with a  $0.5^\circ$  grid (MFWAM05). We note here that Belmadani et al., (2021) also used a nested  $0.1^\circ$  grid (MFWAM01) focusing on the main development region of tropical cyclones. As the finer domain (MFWAM01) southern boundary runs close to the coast of French Guiana, here we used the MFWAM05 grid alone. A  $0.5^\circ$  resolution is sufficient to accurately model the propagation of swell waves across the Atlantic basin, and is of the order of the highest resolutions adopted by existing state-of-the-art global wave models (Morim et al., 2020). In addition, previous MFWAM applications suggested that, despite the higher resolution of the wind forcing, an increased ( $0.5^\circ$  to  $0.1^\circ$ ) grid resolution did not have a significant impact on the model results in deep waters, except for a weak sensitivity of extreme wave conditions (Belmadani et al., 2021).

## 2.4 Method

### 2.4.1 Wave model setup

For the wave model applications, we forced winter wave simulations with the ARPEGE-Climat 6-hourly wind fields obtained from the five members of the three climate experiments introduced in Section 2.1 (Hist-Obs, Hist-Model and RCP-8.5). The use of five-member ensembles for each experiment allows accounting for the uncertainties related to the inherent variability of the climate circulation (Mankin et al., 2020), and increases the robustness of the model results, especially for extreme events (Belmadani et al., 2021; Meucci et al., 2020; Timmermans et al., 2017). Given the computational burden of multiple MFWAM simulations and the study focus on the winter season, we modelled wave conditions ( $H_s$ ,  $T_m$ ,  $D_m$ ) from 1<sup>st</sup> November to 30<sup>th</sup> April (NDJFMA) for 29

following years, for each experiment ensemble. This resulted in 435 time series (3-hourly) of winter wave conditions (Table 2).

We run the historical simulations of wave conditions over the period 1985-2013 and 1984-2012 for the Hist-Obs and Hist-Model experiments, respectively. The former is compared against historical wave data to assess the model accuracy, and the latter is compared to the RCP-8.5 projections to quantify future changes in modelled wave climate. Herein, we analyse and discuss the possible bias in model results against available data as described in Sections 2.4.2, 3.1 and 4.1, although bias correction (e.g. Charles et al., 2012) is not performed (see Section 4.1). The future scenario (RCP-8.5) is run from 2051 to 2079, which corresponds to the latest 29 years of available wind fields from the climate model experience (Section 2.1).

In order to analyze wave climate change offshore of French Guiana, we extracted the MFWAM results over the portion of the domain included between ( $59.5^{\circ}$  -  $48^{\circ}$  W) and ( $2^{\circ}$  -  $12^{\circ}$  N), hereafter referred as MFWAM05\* (Figure 3). As we aim at characterizing the change of deep-water waves, this area extends several hundreds of kilometres offshore of French Guiana's coasts to ensure deep water conditions of the modelled waves. For the analysis of the seasonality of modelled wave conditions (Section 2.4.3), the results are spatially integrated over a part of MFWAM05\* excluding nearshore areas (red region in Figure 3), where waves are strongly affected by complex processes that are not resolved by MFWAM (Anthony et al., 2010). For each experiment, an average 2-D wave field is derived by averaging the results obtained from the five respective ensemble members.

**Table 2.** Summary of the MFWAM simulations including: 6-hourly wind forcing experiments, simulated winter period and time slices, and number of model realizations.

<b>MFWAM model experiment</b>	<b>Simulated time slice</b>	<b>Winter period simulated each year</b>	<b># ensemble members</b>	<b>Total # simulations</b>
Hist-Obs	1985-2013	November 01 – April 30	5	145
Hist-Model	1984-2012	November 01 – April 30	5	145
RCP-8.5	2051-2079	November 01 – April 30	5	145

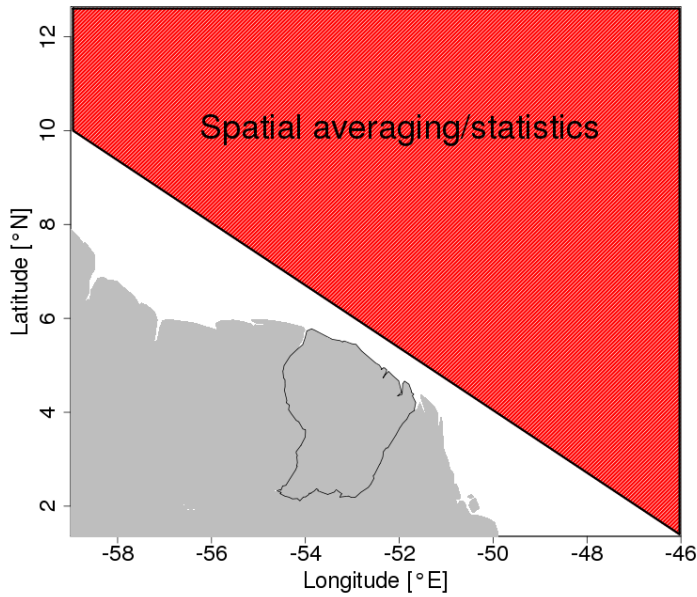


**Figure 3.** Portion of the MFWAM model domain considered for the analysis over the French Guiana region (MFWAM05\*), with a sub-portion (red-shaded area) excluding the coastal band, used to calculate spatial averages and other statistics for the analysis of mean seasonal cycles of modelled wave variables.

#### 2.4.2 Model bias assessment

When addressing future wave climate, it is fundamental to investigate possible biases in model results for a proper interpretation of the projections, especially beyond decadal scale (Bitner-Gregersen et al., 2022; Khandekar, 1989; Lemos et al., 2020). Therefore, as a preliminary step, we compared the wave model results of the Hist-Obs simulation with the available historical data from ERA5, ESA-CCI and wave buoys (Section 2.2).

We remind here that while the MFWAM Hist-Obs simulations are forced with wind data obtained from observed SST fields, each ensemble member is based on different initial conditions and does not ensure a consistent chronology with the observations. This does not allow the quantification of performance metrics derived from the direct comparison of time series (e.g. root-mean-square-error). First, we compared  $H_s$  and  $T_m$  winter mean ( $\overline{H_s^w}, \overline{T_m^w}$ ) and 95<sup>th</sup> percentile ( $H_{s,95}^w, T_{m,95}^w$ ) obtained from the Hist-Obs simulation with ERA5 data over the period 1985-2013 within the MFWAM05\* domain. Then, we interpolated the Hist-Obs results to match the grid of ESA-CCI data and compared the mean and extreme  $H_s$  for the winter season. In this case, extreme  $H_s$  are expressed as monthly exceedance probabilities of four threshold values 1 m, 1.5 m, 2 m, and 3 m, which correspond to the values provided by ESA-CCI (Piollé et al., 2020). Finally, a pointwise analysis is performed for the winter season between the wave buoy data and the Hist-Obs results extracted at the nearest grid points ([52°W; 5°N] for 97304 i.e. 6 km away, and [52.5°W; 5.5°N] for 97303 i.e. 20 km away). For

this comparison, the wave buoy data and 3-hourly model results are represented using box-plots indicating the 25<sup>th</sup>, 50<sup>th</sup> and 75<sup>th</sup> percentiles for  $H_s$  and  $T_m$ , and using wave roses for  $D_m$ .

Ultimately, we also compared the Hist-Obs and Hist-Model simulations to verify the consistency between the two historical ensembles (Section 3.1).

### 2.4.3 Projected winter wave changes

In order to investigate winter wave climate change between the 1984-2012 and 2051-2079 periods in the French Guiana region, we analysed the differences between the RCP-8.5 and Hist-Model ensembles by mapping the evolution of winter wave characteristics (mean  $H_s$  and  $T_m$ , i.e.  $\overline{H_s^w}$  and  $\overline{T_m^w}$ , and median  $D_m$ , i.e.  $D_{m,50}^w$ ) and the respective statistical robustness. The latter is evaluated applying statistical significance tests with control of the False Discovery Rate (FDR) (Benjamini & Hochberg, 1995), which adjusts the resulting *p-values*. The calculation of *p-values* requires the statistical independence of the analysed variables, which we obtained applying a temporal subsampling of the wave data through the computation of decorrelation maps, following the approach proposed by Belmadani et al. (2021) (see Text S2 of Supplementary Material). Finally, the *p-values* are estimated at each model grid point using a Student, Welch or Wilcoxon test based on the probability distribution and variance of the tested variable (Figure S5 of Supplementary Material). This methodology is also applied to the RCP-8.5 and Hist-Model winter  $U_{10}$  fields (Figure 1b) to analyse the projected winter wave climate in light of future changes in the wind forcing. We performed the procedure with the 3-hourly  $H_s$  and  $T_m$ , and the 6-hourly  $U_{10}$  subsampled every 5 days and 10 days, respectively.

The average of instantaneous wave directions ( $\overline{D_m^w}$ ) does not correspond to the mean wave direction  $D_m$  extracted from the winter mean directional wave spectrum and is not necessarily representative of typical wintertime values, introducing potential biases. Compared to  $\overline{D_m^w}$ , the median represents the more frequent  $D_m$  and is less susceptible to biases. Thus, we evaluated the evolution of mean wave direction (rotation) by observing its winter median value ( $D_{m,50}^w$ ) at each grid point across the MFWAM05\* domain. The analysis of directional wave roses at five locations off the French Guiana coast for the Hist-Model and RCP-8.5 experiments suggests that the median represents the real wave rose well, i.e. the wave directions are distributed smoothly (near Gaussian) and do not show multiple peaks that may bias the representativeness of the median (Text S3 of Supplementary Material). Herein, a negative (positive) change in  $D_{m,50}^w$  represents clockwise (counter-clockwise) rotation.

Extremes of the 3-hourly winter wave characteristics are represented here by the respective 10-year return values, obtained from Generalized Extreme Value (GEV) distributions of the annual maxima of the 145 simulated winter seasons for Hist-Model and RCP-8.5. The significance of the estimated changes in extreme values is assessed based on the 95% confidence bounds (2.5<sup>th</sup> - 97.5<sup>th</sup> percentiles)

of the return values (Belmadani et al., 2021) obtained with a bootstrapping of annual maxima (1000 iterations with replacement) and the respective GEVs.

We also estimated the RCP-8.5 return period corresponding to the 10-year Hist-Model return values in order to identify possible increases/decreases in the occurrence frequency of historical 10-year extreme events (Wang et al., 2014).

Further, we analysed the seasonal variability of the projected wave climate by computing the climatological daily means of  $H_s$ ,  $T_m$  and  $H_s^2 T_m$ , spatially averaged over the portion of MFWAM05\* excluding nearshore areas (red area in Figure 3). Herein, we consider  $H_s^2 T_m$  to synthesize the wave energy ( $E$ ). For each calendar date of the winter season (NDJFMA), we estimated the mean of the 145 ( $5 \times 29$ ) values from all the simulated members and years, obtaining an average seasonal cycle of the different variables over the selected area, for the Hist-Model and RCP-8.5 experiments. Then, we applied a 30-day running average to filter out the isolated storm events occurring on intra-monthly time scales.

The seasonal variability of extreme  $H_s$ ,  $T_m$  and  $H_s^2 T_m$  is assessed in a similar fashion as the climatological daily mean values, extracting the spatial maxima over the same portion of MFWAM05\* (red area in Figure 3) at each time step and selecting the daily maximum. This results in 145 values of spatial maxima for each calendar day of the winter season. Then, we evaluate the associated climatological daily exceedance probability, defined as the daily fraction of values (within the sample of 145 values) exceeding a prescribed threshold. We defined the latter threshold by testing several values and retained those that resulted in realistic probability curves, i.e. characterized by a relatively smooth temporal distribution (not too noisy between consecutive days) and a realistic occurrence probability (rare enough for the events to qualify as extremes). Finally, we smoothed the seasonal cycles applying a 30-day running mean.

### 3 Results

The MFWAM model produced 3-hourly series of  $H_s$ ,  $T_m$  and  $D_m$  throughout the winter season (1<sup>st</sup> November to 30<sup>th</sup> April) for 29-year periods under three experiments (Hist-Obs, Hist-Model and RCP-8.5), each one including five ensemble members. The following subsections illustrate the comparison between modelled wave conditions and available data over the historical period 1985-2013 (Section 3.1), as well as the MFWAM winter wave changes projected for 2051-2079 (Section 3.2).

#### 3.1 Model performance

The comparison between Hist-Obs results and ERA5 (Section 2.2.1), wave buoys and ESA-CCI data (Section 2.2.2) provides an indication of the MFWAM model performance in representing mean and extreme historical winter wave conditions over the 1985-2013 period. Figure 4 shows the differences between Hist-Obs and ERA5 fields of wintertime mean and 95<sup>th</sup> percentile  $H_s$  (Figure 4a,b) and  $T_m$



(Figure 4c,d) over the MFWAM05\* domain, and the ERA5 reference values (black contours). The ERA5  $\overline{H_s^w}$  and  $\overline{T_m^w}$  fields reach 2.2 m and 8.0 s, respectively, and both decrease from the northeastern end of the domain to the French Guiana coasts (Figure 4a,c). A similar pattern is observed for  $H_{s,95}^w$  and  $T_{m,95}^w$ , which decrease from 3 m and 10 s to 2-2.5 m and  $\sim 9$  s (Figure 4b,d). Hist-Obs produces a northeast to southwest decrease in  $\overline{H_s^w}$  and  $\overline{T_m^w}$  consistent with ERA5 data (not shown). The model results show an overall underestimation of  $\overline{H_s^w}$  ( $\sim 0.15$  m, i.e.  $\sim 10\%$ , on average), with well represented extremes showing a mild overestimation of 0.1-0.2 m (5-7%) and underestimation of  $\sim 0.1$  m ( $\sim 5\%$ ) in the northwestern and southeastern areas of the domain, respectively (Figure 4a,b). In contrast, the model generally overestimates  $T_m$  over the domain with biases of the order of 0.5-0.8 s (5-10%) for the winter mean values and 10-15% for the extremes (Figure 4c,d).

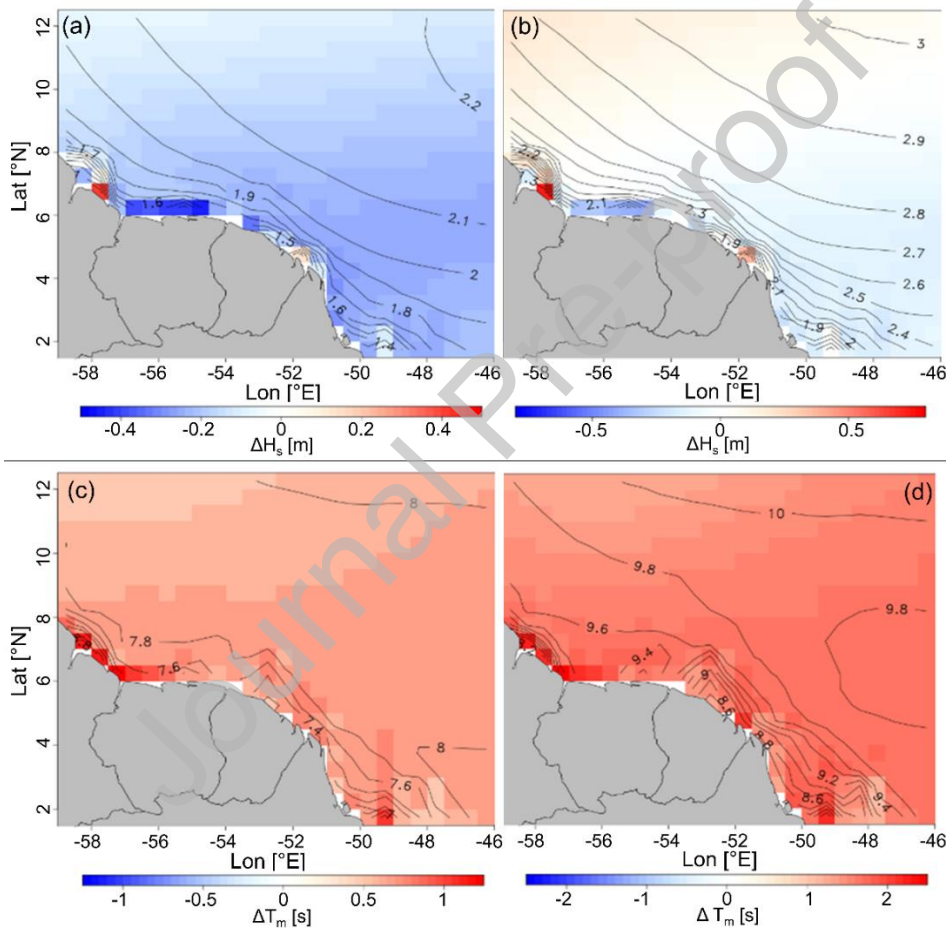


**Figure 4.** Comparison between Hist-Obs and ERA5 winter wave conditions (Hist-Obs minus ERA5) over the 1985-2013 period, including changes in: (a) winter mean  $H_s$  ( $\Delta\overline{H_s^w}$ ); (b) 95<sup>th</sup> percentile  $H_s$  ( $\Delta H_{s,95}^w$ ); (c) winter mean  $T_m$  ( $\Delta\overline{T_m^w}$ ); and (d) 95<sup>th</sup> percentile  $T_m$  ( $\Delta T_{m,95}^w$ ). Black iso-contours indicate the reference ERA5 values.

Compared to ESA-CCI data, the Hist-Obs  $\overline{H_s^w}$  shows a larger bias than the one observed against ERA5, with an overall underestimation of 0.3-0.4 m (20-30%) (Figure 5a). The results show a smaller bias and  $\overline{H_s^w}$  overestimation in the coastal areas north and south from French Guiana, although both ESA-CCI and MFWAM data are highly uncertain in nearshore zones (as stated in

Section 2). The probability of  $H_s$  exceeding 2 m or 3 m (extreme waves) is consistent between Hist-Obs and ESA-CCI, with a decay in the occurrence of  $H_s > 2$  m and  $H_s > 3$  m as waves approach the continent (Figure 5b, 5c). However, Hist-Obs results in a slightly more gradual decay (milder gradients) than ESA-CCI 2- and 3- m exceedance probability across the MFWAM05\* domain (Figure 5b,c). Such difference is also observed for lower thresholds of exceedance (1 m and 1.5 m), as shown in Figure S7 of Supplementary Material.

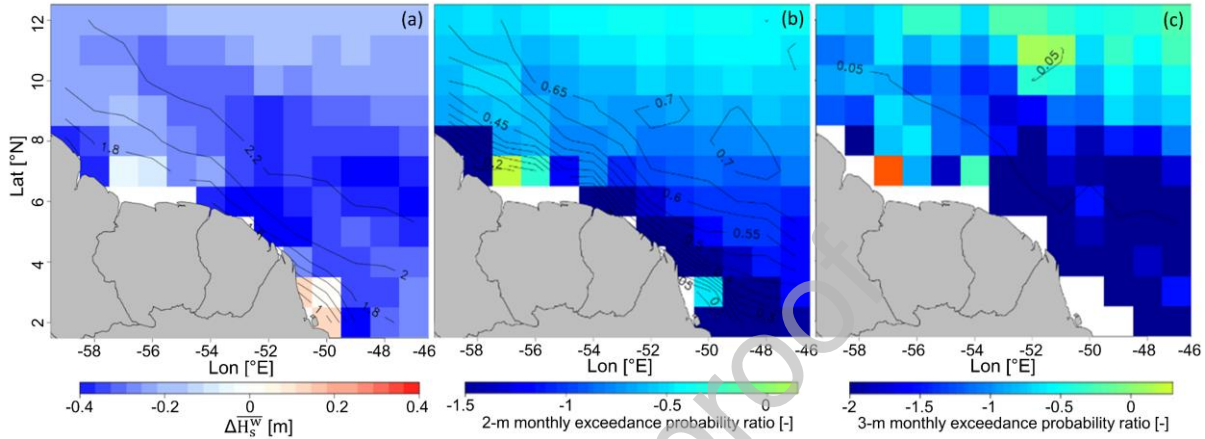


**Figure 5.** Comparison between Hist-Obs and ESA-CCI winter wave conditions over the 1991-2013 period, including differences in: (a) winter mean  $H_s$  ( $\Delta\overline{H_s^w}$ , Hist-Obs minus ESA-CCI); (b) 2-m and (c) 3-m monthly exceedance probability, expressed as the ratio (Hist-Obs/ESA-CCI) of probabilities on a power (base 2) scale, i.e. -0.05 corresponds to  $2^{-0.05} \sim 0.966$ . Black iso-contours indicate the reference ESA-CCI (a)  $\overline{H_s^w}$  values and (b) probabilities.

The analysis of MFWAM performance is complemented by comparing the Hist-Obs results with *in situ* data from coastal wave buoys (Section 2.2.2). The 97304 buoy data and the nearest model results ( $52^\circ\text{W}$ ;  $5^\circ\text{N}$ ) show nearly matching values of the median winter  $H_s$  ( $H_{s,50}^w \sim 1.32$ - $1.33$  m), though with a narrower confidence interval for the model results, which overestimate and underestimate the 25<sup>th</sup> and 75<sup>th</sup> percentiles, respectively, by  $\sim 8\%$  (Figure 6a,b). In respect to the 97303 buoy, located in the vicinity of Kourou (Figure 2a), the nearest model predictions ( $52.5^\circ\text{W}$ ;  $5.5^\circ\text{N}$ ) overestimate the median winter  $H_s$  ( $H_{s,50}^w \sim 1.39$  m vs 1.22 m) and the 25<sup>th</sup> percentile ( $H_{s,25}^w \sim 1.16$  m vs 1.02 m) by  $\sim 14\%$ , and underestimates the 75<sup>th</sup> percentile ( $H_{s,75}^w \sim 1.66$  m vs 1.72 m) by  $\sim 3\%$  (Figure 6c,d). The 25<sup>th</sup> and 75<sup>th</sup> percentiles, and median values of  $T_m$  are very consistent with differences of 1-2% off Cayenne (Figure 6c,d) and  $<1\%$  off Kourou (Figure 6c,d). The agreement with winter wave data from the buoys provides a good validation of the model, considering that the Hist-Obs climate simulations are forced with observed monthly SSTs without any data assimilation in the wave model or its wind forcing.

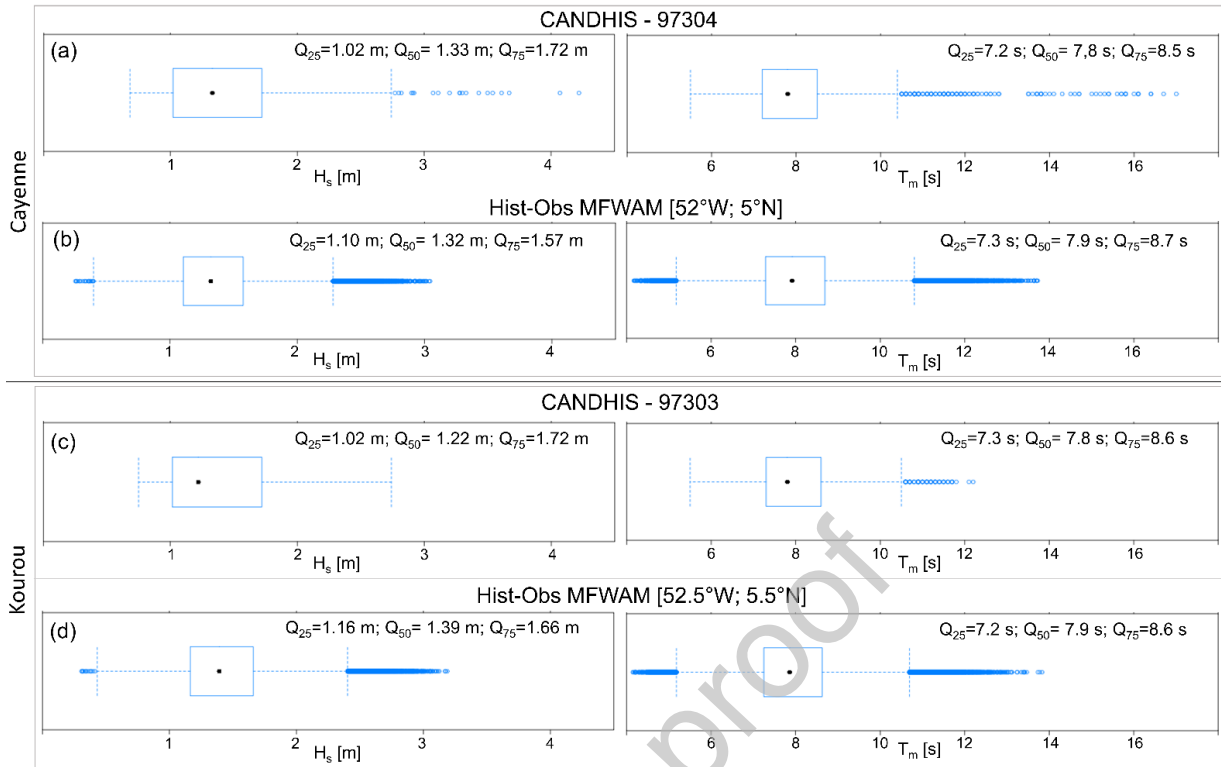


**Figure 6.** Box plots (25<sup>th</sup>, 50<sup>th</sup> and 75<sup>th</sup> percentiles) of  $H_s$  and  $T_m$  from (a) the CANDHIS 97304 buoy and (b) Hist-Obs [52°W; 5°N] MFWAM grid point near Cayenne; and (c) the CANDHIS 97303 buoy and (d) Hist-Obs [52.5°W; 5.5°N] MFWAM grid point near Kourou.

The wave roses representing the buoy records offshore of Cayenne (97304) and Kourou (97303) both show an incident direction of winter waves primarily from the NE (>50%) and NNE (~35%) sectors, with most of the largest waves ( $H_s > 2$  m) coming from the NE sector (Figure 7a,c). Consistently, the modelled winter waves and their extremes at the two nearest grid points mainly come from the NE (>60%). On the other hand, in both locations, less than 20% of modelled waves come from the NNE sector and include only waves up to 1.8 m (Figure 7b,d). Offshore of Cayenne, this difference is mostly compensated by more waves falling into the NE sector, while near Kourou it is evenly distributed in the neighbour directional sectors (NNE and ENE) (Figure 7b,d). Both buoys also recorded ~10% of waves (up to 1.8 m) coming from the N sector, which do not appear in the model results. Hence, both comparisons offshore Cayenne and Kourou suggest a mild clockwise bias of the model.

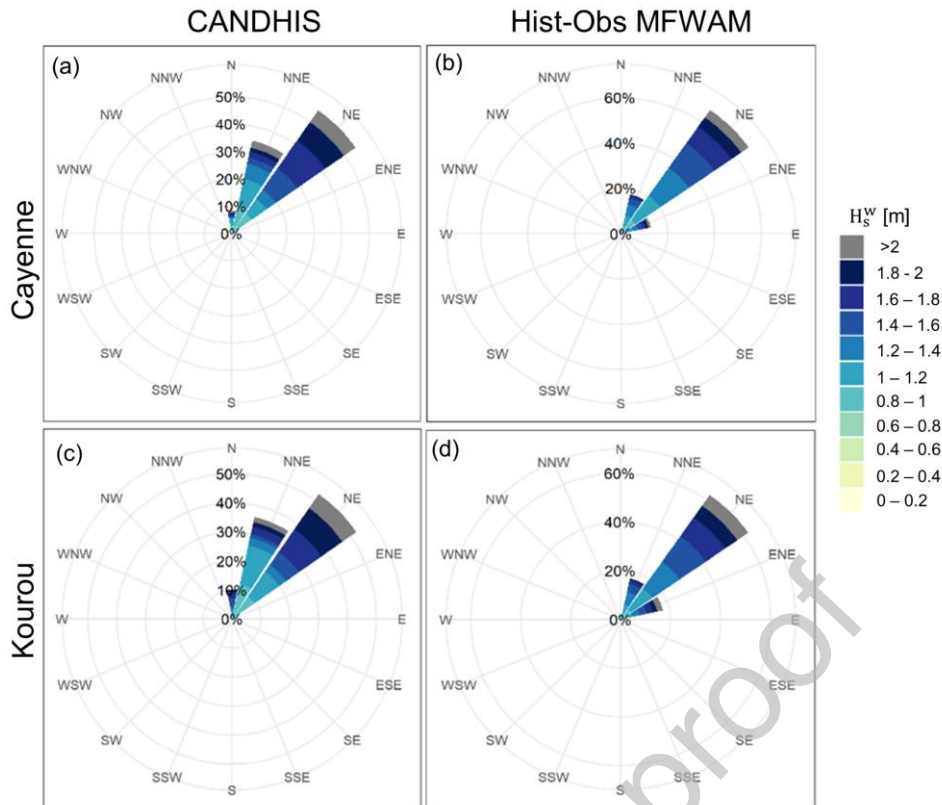


**Figure 7.** Wave roses of winter conditions offshore of: Cayenne from (a) the 97304 wave buoy, and (b) Hist-Obs [52°W; 5°N]; and Kourou from (c) the 97303 wave buoy and (d) Hist-Obs [52.5°W; 5.5°N], with colour scale indicating different ranges of winter  $H_s^w$ .

The Hist-Obs and Hist-Model results over the 1985-2012 period show notable differences mainly in the mid-high latitudes, corresponding to a westward shift of winter mean and extreme  $H_s$  in the Hist-Obs experiment (Figures S8 of Supplementary Material). However, in the tropical latitudes and French Guiana region the two experiments reproduce the same overall wintertime wave climate (Figure S9 of Supplementary Material), consistently with the outcomes of Chauvin et al. (2020) and the summertime comparison performed by Belmadani et al. (2021) over the Atlantic Ocean.

Overall, despite some biases between the Hist-Obs experiment and the three reference datasets, and recalling the uncertainties and limitations affecting reanalysis, satellite and buoy data, it is concluded that the model reproduces fairly well the winter wave climate in the study area over the historical period. This, together with the agreement between the Hist-Obs and Hist-Model experiments (Section 2.4.2), confirms the MFWAM suitability to evaluate future changes in winter wave climate offshore of French Guiana.

### 3.2 Winter wave projections

The future wave projections from RCP-8.5 (2051-2079) and the historical wave conditions from Hist-Model (1984-2012) are used to derive projected changes of the winter wave climate off the coasts of French Guiana in the RCP-8.5 scenario. Figure 8a,b show that the model predicts a

statistically significant reduction (3-5%) of  $\overline{H_s^w}$  and  $\overline{T_m^w}$  over the whole study area (MFWAM05\*) by 2051-2079. The projected changes in mean  $\overline{H_s^w}$  ( $\overline{T_m^w}$ ) are larger in the northern (coastal) area of the domain, and gradually decrease towards (away from) the French Guiana coast (Figure 8a,b). The modelled historical (Hist-Model) winter waves show a rather homogeneous spatial pattern of  $D_{m,50}^w$  (black arrows in Figure 8c), characterized by median direction mostly from the NE, turning towards ENE in the northwest area of the domain and NNE in the southeast. Figure 8c also shows an overall projected clockwise rotation between  $1^\circ$  and  $3^\circ$  of winter wave angle, with larger changes in the northwestern area of the domain and smaller changes in the southeast, accentuating the spatial variability of  $D_{m,50}^w$ . The examination of wave roses extracted from the RCP-8.5 and Hist-Model results at five locations confirm that the median of  $D_m$  well represents the actual incident wave direction offshore of French Guiana (Text S3 of Supplementary Material).

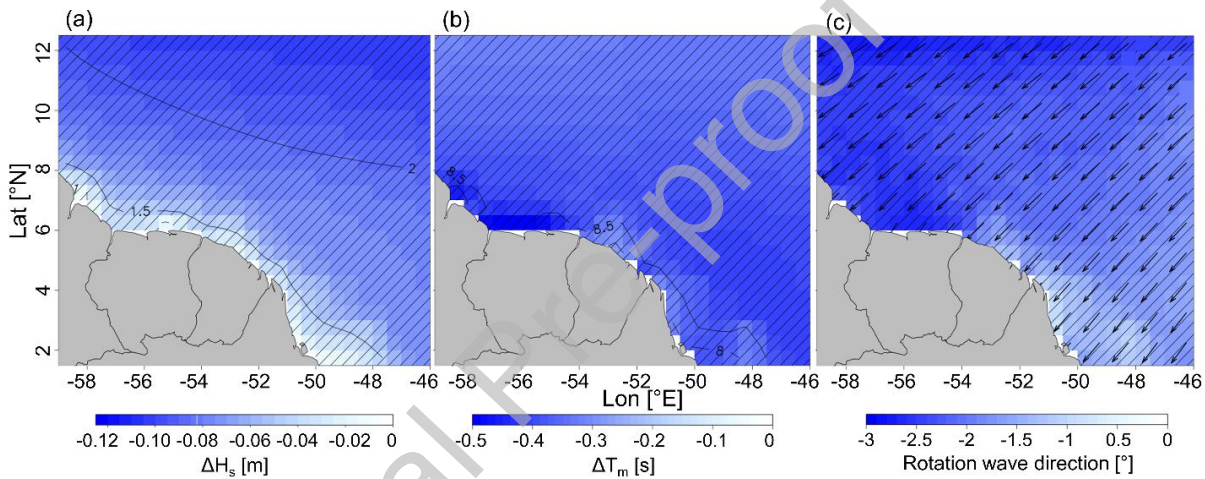


**Figure 8.** Projected changes in winter mean wave climate (2051-2079) for the RCP-8.5 scenario relative to Hist-Model historical conditions (1984-2012), including: (a)  $\Delta\overline{H_s^w}$  and (b)  $\Delta\overline{T_m^w}$  with black contours indicating the reference Hist-Model values and hatchings indicating statistically significant changes (using p-values and control of False Discovery Rate, Section 2.4.3); and (c)  $\Delta D_{m,50}^w$  with arrows indicating the reference Hist-Model wave directional pattern. Negative  $\Delta D_{m,50}^w$  indicate clockwise rotation.

For the Hist-Model experiment, the 10-year return values of  $H_s$  ( $T_m$ ) vary between 3 m (13.5 s) a few tens of kilometres off the coast, and  $>4.2$  m ( $>15.5$  s) in the northern area of the domain as shown in Figure 9a (Figure 9b). The historical extreme values of  $E$  show similar contours as  $H_s$ , with magnitudes ranging between  $50 \text{ m}^2\text{s}$  and  $250 \text{ m}^2\text{s}$  (Figure 9c). The simulated future winter wave climate (RCP-8.5) shows an overall 5% decrease in 10-year return  $H_s$ , which is stronger and statistically significant in the northwestern to central area of the domain (7-8%) and smaller near the coasts and in the southeastern part of the domain (3-4%, Figure 9a). For the extreme  $T_m$ , the projections show a small increase (1-2%) in the northeast, and a decrease of the order of 3-4% towards the coasts, although these changes are statistically significant only in over a small part of the southeastern coastal region (Figure 9b). An overall decrease of  $\sim 10\%$  in the derived extreme  $E$  is

projected, with changes statistically significant in the central portion of the domain (where projected change reach 15%) and in isolated coastal areas off French Guiana (Figure 9c). Figure 9d-f shows the RCP-8.5 projected return periods corresponding to the Hist-Model 10-year return values for  $H_s$ ,  $T_m$  and  $E$ . For  $H_s$ , the historical 10-year return values are projected to be associated with a return period ranging from 15 years at the French Guiana coast, up to 35-40 years in the western part of the domain (Figure 9d). The future return periods for the historical decadal  $T_m$  values gradually increase from the northeastern end of the region ( $\sim 10$  years) to the coasts ( $\sim 20$  years, Figure 9e). For wave energy, future return periods grow up to 15-25 years, peaking in the central-western part of the domain (Figure 9f).

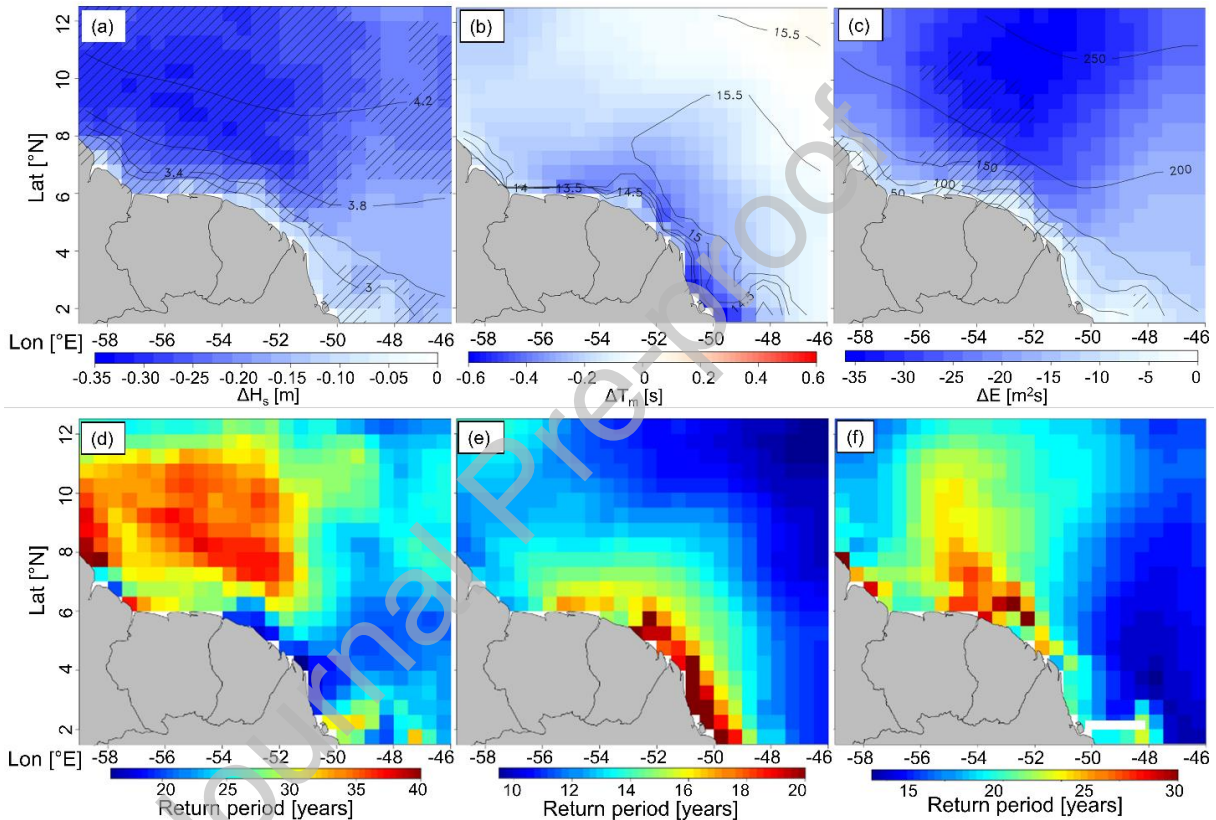


**Figure 9.** Projected changes in (a-c) 1 in 10 years winter waves for the RCP-8.5 (2051-2079) scenario relative to Hist-Model historical (1984-2012) conditions, illustrating the evolution of extreme values for: (a)  $H_s$ , (b)  $T_m$  and (c)  $E=H_s^2T_m$ ; and (d-f) future RCP-8.5 return periods (years) corresponding to the Hist-Model (1984-20123) 10-year return (d)  $H_s$ , (e)  $T_m$ , and (f)  $E$ . Black contours indicating the reference Hist-Model values and hachings indicating statistically significant changes (using p-values and control of False Discovery Rate, Section 2.4.3).

Figure 10 shows the seasonal variability of historical and projected mean wave characteristics and the respective exceedance probabilities within the winter season (NDJFMA). Between November and February, the historical climatological daily mean  $H_s$  and  $H_s^2T_m$  gradually increase from 1.5 m to 2.2 m and from 25  $m^2s$  to 50  $m^2s$ , respectively, and then decrease to  $H_s=1.9$  m and  $H_s^2T_m=30$   $m^2s$  by April (Figure 10a,c). In contrast, in the beginning of the season, the daily mean  $T_m$  undergoes a rapid growth (within a few days) from 8.6 s to 9.2 s, followed by a gradual decrease to 8.8 s by March, and

an accelerated decrease to 8.2 s by April (Figure 9b). Figure 9a,b indicates that the statistically significant decrease observed for  $\overline{H_s^w}$  and  $\overline{T_m^w}$  (Figure 8a,b) persists evenly throughout the winter season. Consequently, the daily mean energy (E) exhibits a similar trend, although with enhanced projected decrease at the season peak, in January-February (Figure 9c).

Figure 10d-f illustrates the probabilities that the climatological wintertime daily maxima of historical and future modelled  $H_s$ ,  $T_m$  and E exceed 3.5 m, 13 s, and  $110 \text{ m}^2\text{s}$ , respectively. All the analyzed variables exhibit an overall reduction of exceedance probability of the respective thresholds, which is consistent with the projected changes observed for the 10-year return values (Figure 9). The projected probabilities for  $H_s$  and E are the highest in the second half of January compared to the longer period (early January to mid-February) observed in the Hist-Model experiment, with a  $\sim 30\%$  decrease for both parameters (Figure 10d,f). The peak occurrence probability of future  $T_m$  extremes decreases by 35-40% (from  $\sim 0.08$  to  $\sim 0.05$ ) and remains stable between November and February, as per the historical simulation, although with a predicted drop in December-January (Figure 10e).

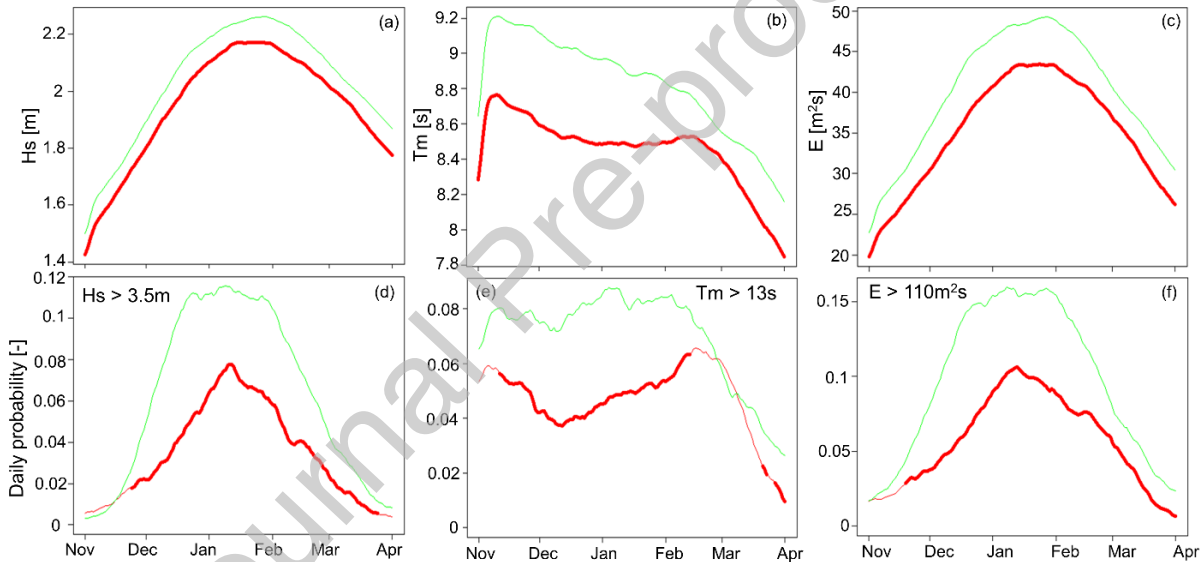


**Figure 10.** Seasonal variability (in winter) of climatological daily mean (a)  $H_s$ , (b)  $T_m$ , and (c)  $H_s^2 T_m$ , and daily probability of exceeding (d) 3.5 m for  $H_s$ , (e), 13 s for  $T_m$ , and (f)  $110 \text{ m}^2\text{s}$  for  $H_s^2 T_m$ , including Hist-Model historical (green curves) and projected RCP-8.5 data (red curves). Bold red lines indicate statistically significant ( $p < 5\%$ ) projected changes.

## 4 Discussion

### 4.1 Model performance

The Hist-Obs results over the French Guiana region showed a general underestimation of the winter mean significant wave height compared to ERA5 reanalysis and ESA-CCI satellite data (Section 3.1). Moreover, the model shows larger differences against ESA-CCI data (20-30%) than against ERA5 ( $\sim 10\%$ ). This appears consistent with the tendency of ERA5 reanalysis to underestimate  $H_s$ ,

observations in the North Atlantic basin (Hawkins et al., 2022; Timmermans et al., 2020), although ESA-CCI data is also affected by uncertainties due to the sampling frequency and data processing.

In a recent assessment of global wave model skill against ERA5 wave data, the 1979-2004 average  $H_s$  from two wave models forced with CMIP6 GCMs exhibited mild positive biases (<10% overestimation) in the French Guiana region (Meucci et al., 2023). Interestingly though, over the 1985-2014 period, one of the models (forced with the EC-Earth GCM) showed a statistically significant decreasing trend in annual mean  $H_s$  near French Guiana, in contrast to the ERA5 statistically significant increasing trend, both larger than 1.75%/decade (Figure 12 of Meucci et al., 2023). Consequently, over the 1985-2014 period, this wave model tends to increasingly underestimate the ERA5 annual mean  $H_s$  data offshore of French Guiana, supporting the findings of our comparison for the wintertime season (Section 3.1). The second CMIP6-driven model (forced with the ACCESS-CM2 GCM) also produced a decreasing  $H_s$  trend in the French Guiana region, although not statistically significant.

MFWAM performs better in reproducing extreme  $H_s$ , with biases generally <7%. The source of this bias may be attributed (at least partially) to the surface wind speed ( $U_{10}$ ) produced by ARPEGE-Climat, which underestimates the ERA5 data both in the tropics (by up to 1.5 m/s off French Guiana) and north of 50°N (by up to 2-2.5 m/s) (see Figure 1a and S9). In addition, the model reproduces very well the mean  $H_s$  conditions measured by the wave buoys offshore of Cayenne and Kourou, with much weaker negative biases.

MFWAM also proved to have good skills in reproducing the wintertime mean wave period, with excellent performances relative to wave buoy data, and a relatively small bias against ERA5 estimates (10-15% overestimation). In terms of median  $D_m$ , the model features a systematic, though small, clockwise rotation compared to the buoy wave roses. While the latter bias may be partly related to a corresponding bias in the forcing wind fields, which show a slight clockwise difference against ERA5 winds (Figure S11b of Supplementary Material), the origins of the mild biases in  $T_m$  is not straightforward.

Overall, despite the presence of some biases, the model performs well over the historical period, thus supporting the application of MFWAM for the simulation of future winter wave climate. However, further assessment of the model performance and the application of bias correction methods to the wave projections require the development of long uninterrupted wave data from measurements or extensively validated hindcasts (e.g. Charles et al., 2012).

## 4.2 Wave climate change

### 4.2.1 Projected winter wave changes

The MFWAM RCP-8.5 experiment results predict an overall negative trend in winter mean  $H_s$  and  $T_m$  as well as a slight clockwise rotation of  $D_{m,50}^w$  in the French Guiana region by the 2051-2079 period. This appears to be in contrast with the projected intensification of wind speed and the



counter-clockwise rotation of the northeasterly trade winds (Section 2.1). However, the general decrease observed for  $\overline{H_s^w}$  and  $\overline{T_m^w}$  in the French Guiana region can be explained by the larger-scale signal of modelled wave conditions. In fact, an analysis of the model results over the North Atlantic basin reveals a basin-wide reduction, the strongest decrease in  $\overline{H_s^w}$  occurring around 60°N and 30-40°N, thereby reducing the historical gradients between the larger mid-latitude waves and the smaller tropical waves (Figure 11a). Such  $\overline{H_s^w}$  changes are most likely linked to an overall weakening of the mid-latitude future winds (Figure 1b) and to those weather types (synoptic patterns) that associate weaker storms along the mid-to-high latitudes, which are projected to become more frequent during winter (Lemos et al., 2021).

As North Atlantic swells are the dominant component of sea states approaching the French Guiana coasts in the winter season (Anthony et al., 2011; Young, 1999), the weakening of such swells may be identified as the main driver of projected changes in  $\overline{H_s^w}$  offshore of French Guiana compared to wind sea. However, the increase in wind speed projected for the RCP-8.5 scenario over the tropical band (Figure 1b) may contribute to the attenuation of  $\Delta\overline{H_s^w}$  (decrease) equatorward from 30°N (Figure 11a). In contrast, the modelled changes in  $\overline{T_m^w}$  are more pronounced south of 30°N, near the west-African and South-American coasts, including the French Guiana region (Figure 11b). The stronger reduction in  $\overline{T_m^w}$  over the latter area is located on the edge of the signal observed for the main changes in  $\overline{H_s^w}$ , suggesting that these two variables are linked by the southwards propagation of North Atlantic swells. Indeed, if North Atlantic swells are reduced in the future, the wave dispersion in deep water will drive a decrease in  $\overline{T_m^w}$  that intensifies with distance from the source.

The trends featured in our winter projections between 1984-2012 and 2051-2079 in the French Guiana region are consistent with the COWCLIP winter projections between 1979-2004 and 2080-2099, with  $\overline{H_s^w}$ ,  $\overline{T_m^w}$  and  $D_{m,50}^w$  changes falling in the respective ranges of values predicted by the multi-model ensemble (Section 4.2.3).

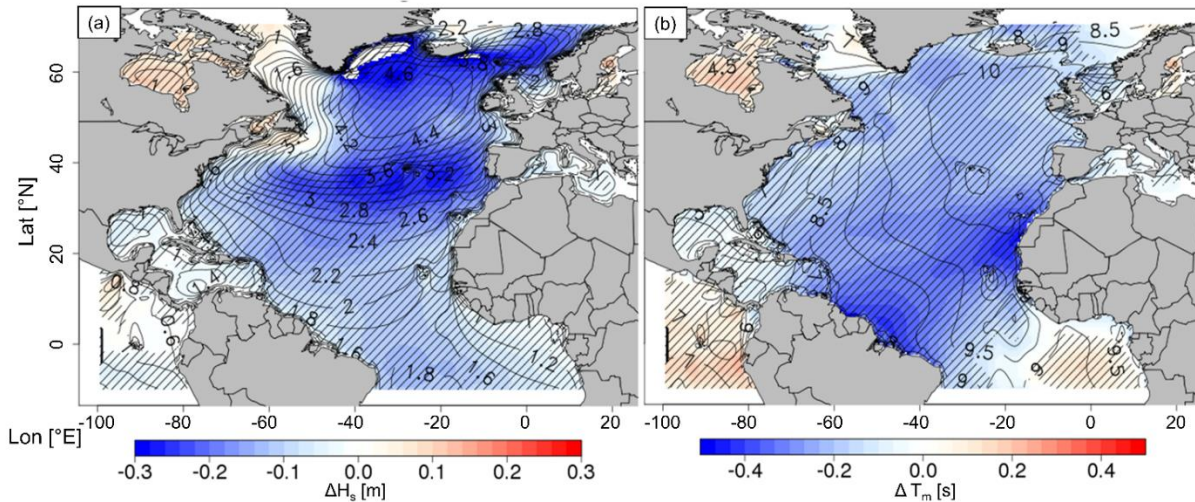


**Figure 11.** Projected changes in winter mean wave climate for the RCP-8.5 scenario (2051-2079) relative to Hist-Model historical conditions (1984-2012) over the North Atlantic basin: (a)  $\Delta H_s^w$  and (b)  $\Delta T_m^w$ , with black contours indicating the reference Hist-Model values and hatchings indicating statistically significant changes.

The analysis of 10-year return values for wave height, period and energy suggests that current winter extremes will occur more rarely in the future (Figure 9), and will be more concentrated around the month of January (Figure 10). Indeed, the historical (Hist-Model) 10-year events are projected to associate return periods between 15 and 40 years in the future (RCP-8.5). This is in line with existing global projections, which predicted an overall annual decrease in 20-year (Lobeto et al., 2021) and 100-year (Meucci et al., 2020) return  $H_s$  by the end of the 21<sup>st</sup> century for the RCP8.5 scenario in the North Atlantic basin. While the results of the latter studies are associated with low statistical significance near French Guiana (Lobeto et al., 2021; Meucci et al., 2020), the statistical significance of our projections provide more confidence to the predicted trends. However, our projected extremes may still present some uncertainties, e.g. stemming from the uncertainties affecting future extratropical storm tracks (Lobeto et al., 2021; Meucci et al., 2020).

#### 4.2.2 Seasonality of wave climate change

Our winter wave projections are complementary to Belmadani et al. (2021)'s projections of summer-fall wave climate (hurricane season) over the Atlantic basin, which are based on the same modelling framework. The summer-fall season simulations (Figure 5b,c of Belmadani et al. 2021) showed a statistically significant decrease in seasonal mean  $H_s$  over the French Guiana region, and in seasonal mean  $T_m$  near French Guiana's coast (and non-statistically-significant increase offshore), both at rates similar to the ones obtained from our winter projections, resulting from changes in large-scale patterns. The latter lead to an overall mean reduction of 5-10% in  $H_s$  and ~5% in  $T_m$  throughout most of the year near French Guiana coast. We note here that the summer-fall (July - November) and winter (November - April) projections do not include the May - June period. On a larger scale, this is in line with the outcomes of previous studies, which obtained the same order of decrease in annual

mean  $H_s$  by 2100 over the North Atlantic region for the RCP-8.5 scenario (Bricheno & Wolf, 2018; Charles et al., 2012). Similar trends, though with different intensities (0-7% decrease), were observed also by Meucci et al., (2023) across the Atlantic Ocean for a similar greenhouse gas concentration scenario.

Similarly to our modelled changes of 10-years return winter wave events (Figure 9), Belmadani et al. (2021) also projected a decrease in extremes during the summer-fall season over the Atlantic Equatorial region by 2051-2080, though of lower magnitude and statistically significant only near the coast. The Authors attributed this change to a poleward migration of extreme wave heights in response to the associated summertime tropical cyclone activity. Instead, the decrease of 10-years  $H_s$  projected near French Guiana during the winter season is mostly driven by a decrease in extreme wind-wave significant height ( $H_{s0}$ ) over the mid- and high-latitudes (20°N-30°N), and the consequent decrease in significant height of primary swells ( $H_{s1}$ ) coming from the North (Figure S10 of Supplementary Material).

#### 4.2.3 COWCLIP multi-model projections

The COWCLIP projections indicate a statistically significant clockwise change in annual mean  $D_m$  of  $\sim 1^\circ$  in the northern coastal area of French Guiana (Figure 3 of Morim et al., 2019), which is in line with the MFWAM results for the wintertime season (Section 3.2). Further north, along the Surinam coast, COWCLIP also predicts a statistically significant decrease in annual mean  $T_m$  (Figure 3 of Morim et al., 2019), which, given the relatively coarse resolutions of the ensemble members, may extend to the French Guiana region. This is consistent with the combined MFWAM summertime and wintertime projections offshore of French Guiana (Section 4.2.2).

We further investigate the annual and monthly averages of COWCLIP wave projections at the interpolated grid point (see Text S4 of Supplementary Material) closest to the French Guiana coast (52°W; 6°N) for the RCP4.5 and RCP8.5 scenarios. This allowed a qualitative comparison with the MFWAM winter projections, and the investigation of the marginal (scenario-based) uncertainties associated with future greenhouse gas emissions, as well as uncertainties in climate model and wave modelling approach (Morim et al., 2019). The projected changes in  $H_s$ ,  $T_m$  and  $D_m$  are estimated as the difference of the respective annual and monthly averages between 2081-2099 and 1979-2004, for each available climate-wave model combination of the ensemble (Table S1 of Supplementary Material). It is worth noting that, unlike our analysis, COWCLIP considers the changes in mean  $D_m$  and not its median value. For each ensemble of projections (and for both annual and monthly means), we estimate the 95% confidence interval (2.5<sup>th</sup> - 97.5<sup>th</sup> percentiles) of the ensemble mean by applying an empirical bootstrapping method (1000 iterations).

The multi-model ensemble predicts larger changes in wave characteristics for the RCP8.5 scenario compared to RCP4.5 for both annual and monthly means (Figure 12), suggesting that the respective uncertainties are mostly driven by the combination of GCM and wave model. This corroborates the

findings of Morim et al. (2019)'s investigation of the relative contributions of uncertainties in RCP scenario, GCM and wave model (including their interactions), to the COWCLIP projection total uncertainties (Morim et al., 2019).

The monthly changes show an overall reduction in  $H_s$  and  $T_m$ , with stronger changes from December to April (winter) for both RCP4.5 and RCP8.5 scenarios, while the monthly mean  $D_m$  is predicted to rotate clockwise throughout the year (Figure 12d-f). Although the monthly changes in  $H_s$  and  $T_m$  remain negative across the respective confidence intervals between December and March, some ensemble members yet predict opposite trends (positive) over this period (Figure 12d,e). Meanwhile, the monthly confidence interval of projected  $D_m$  always includes positive (counter-clockwise) values of modelled rotation, although with a strong asymmetry towards negative (clockwise) values (Figure 12f). Hence, an increase in  $H_s$  and  $T_m$ , and/or a counter-clockwise rotation of  $D_m$  cannot be excluded, undermining the robustness of the COWCLIP projections at this location and confirming (Morim et al., 2019) results.

Nonetheless, while uncertain, the COWCLIP projections are in line with the MFWAM projections discussed herein (Sections 4.2.1 and 4.2.2), providing a qualitative validation of our projected trends. Indeed, despite the different time slices being considered, for the RCP8.5 scenario the wintertime (NDJFMA) ensemble mean COWCLIP projected changes in  $H_s$ ,  $T_m$  and  $D_m$  are of the order of -3%, -4% and  $\sim 1^\circ$  clockwise, respectively, against -3-5%, -3-5% and  $1-3^\circ$  clockwise for MFWAM.

The choice between a dynamic or statistical downscaling approach does not seem to have a significant impact on the uncertainties (ensemble confidence interval) for the changes in monthly mean  $H_s$  (Text S4 of Supplementary Material). In fact, Figure 12d shows that the statistically downscaled members (ECCC-s) are well distributed within the range of modelled results in the winter months.

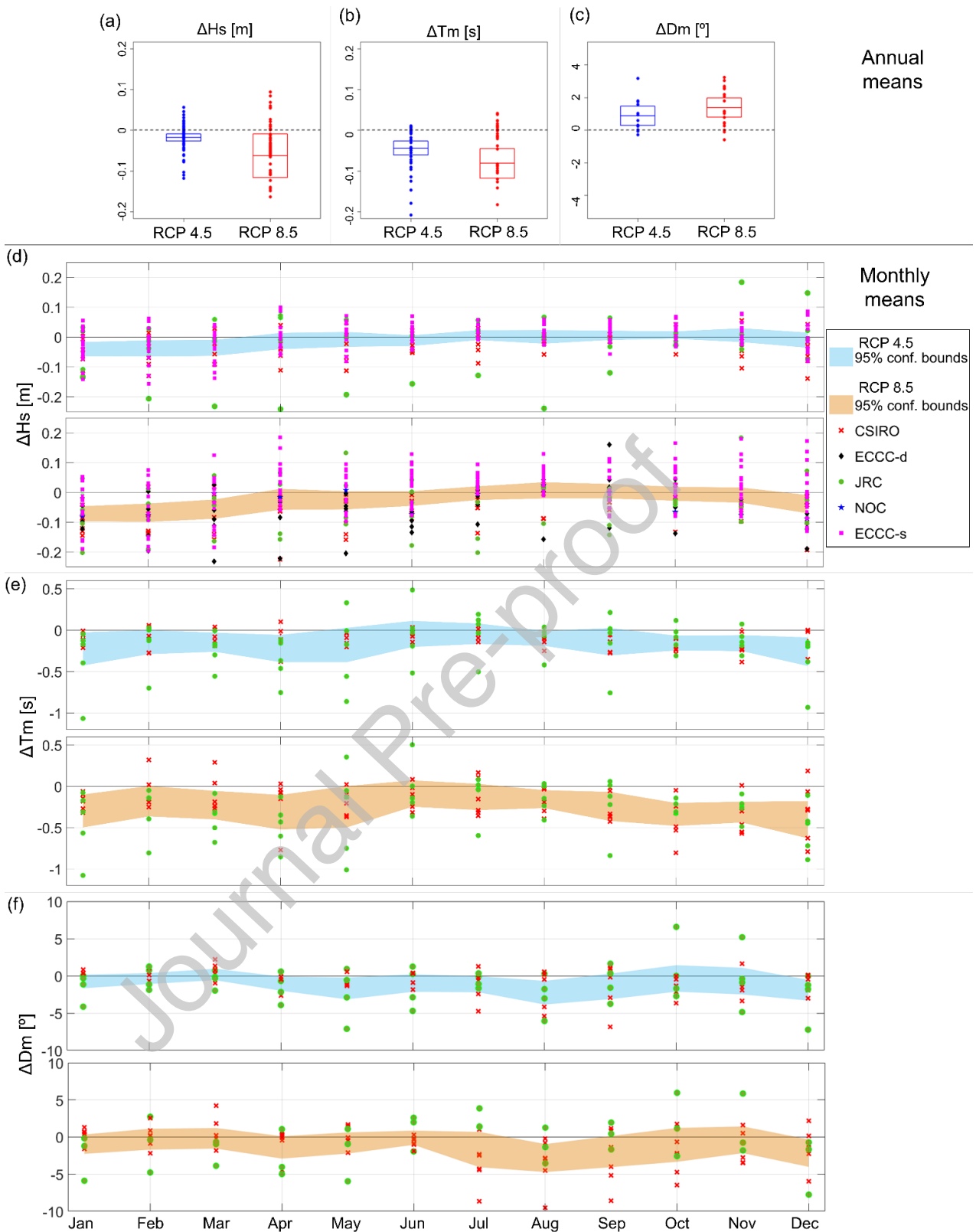


**Figure 12.** COWCLIP 2081-2099 ensemble projections relative to 1979-2004, including projected changes in annual (a-c) and monthly means (d-f) of (a,d)  $H_s$ , (b,e)  $T_m$  and (c,f)  $D_m$ , for the RCP4.5 (blue) and RCP8.5 (red) scenarios, extracted at the nearest grid point to French Guiana ( $52^\circ\text{W}$ ;  $6^\circ\text{N}$ ). Box-plots (a-c) indicate the 25<sup>th</sup>, 50<sup>th</sup> and 75<sup>th</sup> percentiles of the ensemble projections. Shaded areas indicate the 95% confidence intervals of ensemble mean values.

### 4.3 Implications for coastal French Guiana

The projected changes in future wave climate may affect the evolution and migration of mud banks, which control the morphodynamics of the French Guiana coast. As mud-bank dynamics respond to the wave-driven longshore currents (Eisma et al., 1991; Lakhan & Pepper, 1997), the expected clockwise rotation of wave direction may reduce the northeast component of the incident power, altering the rates of bank migration. In addition, the largest effects of waves on mud occur during high-energy events that follow extended low-energy periods (Gratiot et al., 2007). Hence, despite the projected decrease in  $\overline{H_s^w}$  and  $\overline{T_m^w}$ , the narrowed period of likely winter extremes in  $H_s$  and in wave energy (more concentrated in January, Figure 10d,f) results in longer calm periods preceding high-energy events, which may lead to increased suspension of sediment from the mud banks. On the other hand, the general decrease in  $\overline{H_s^w}$  of North Atlantic swells (Figure 11a) will likely reduce the resuspension of sediments (Vantrepotte et al., 2013). However, the future evolution of mud-bank dynamics along the coasts of French Guiana also depends on changes in the Amazon River sediment supply and in tidal currents (Anthony et al., 2010; Froidefond et al., 1988; Gardel & Gratiot, 2005). Therefore, the effects of wave climate change on the dynamics of French Guiana mud banks are not straightforward and require further investigation of the concurrent action of waves and other drivers (Vantrepotte et al., 2013).

In terms of coastal hazard, future sea-level rise is already expected to trigger or increase chronic flooding in tropical regions (Le Cozannet et al., 2021), including French Guiana (Longueville et al., 2022; Thiéblemont et al., 2023). Our analysis of future wave climate evolution suggests that the sole effect of waves should not exacerbate flood hazard (assuming no significant impact on mud bank migration), and that considering an unchanged wave climate is a conservative assumption for coastal flood hazard assessment in French Guiana (Longueville et al., 2022). However, neglecting the impact of wave climate change on the migration of mud banks, which can behave as flood defence, is a strong assumption. Therefore, a detailed assessment of future flood hazard in French Guiana requires more local studies accounting for the influence of wave climate change on mud-bank migration.

### 4.4 Assumptions and limitations

Wave modelling is affected by uncertainties related to model calibration, forcing conditions, and parametrization of some physical processes. Such uncertainties can cascade through the assessment of important processes, e.g. future shoreline evolution (D'Anna et al., 2022; Toimil et al., 2021) and coastal flooding (Parodi et al., 2020; Vousdoukas et al., 2018), and affect the support of decision making for coastal adaptation to climate change (Hinkel et al., 2019, 2021). Although based on 5-member ensembles, the projections presented here are based on a single combination of wave model and GCM, which does not allow the quantification and analysis of uncertainties. However, our winter projections may be integrated in future ensemble-based seasonal assessments of wave climate

change, or combined with existing summertime projections and complementary May-June projections (Section 4.2.2) for annual assessments over the Atlantic Ocean, in a similar fashion to the COWCLIP ensemble (Morim et al., 2019).

The wave projections presented here did not undergo any model bias correction. The application of bias correction methods, such as *quantile-quantile* corrections (Déqué, 2007) is becoming a common practice in the context of wave climate modelling (Casas-Prat et al., 2024; Charles et al., 2012; Lemos et al., 2020, 2024; Lira Loarca et al., 2023), and can help reducing the uncertainties in future projections, including those for extreme waves (Lobeto et al., 2021; Meucci et al., 2020; Morim et al., 2023). Such methods require long and reliable time series of wave conditions (long enough to capture the main modes of the local wave climate variability), which then constitute a reference dataset for the comparison with historical model simulations in order to derive parametrized ‘correction formulae’. The historical wave datasets currently available for the French Guiana region are not suitable to be used as references for bias correction. Indeed, ERA5 underestimates the wave variables in the Atlantic Ocean, ESA-CCI satellite data is available at monthly frequency and only provide  $H_s$  measurements, and the CANDHIS buoy data cover relatively short periods with multiple gaps. Yet, the current model results provide state-of-the-art wave projections, and the application of bias corrections are advised in future research, as appropriate datasets will become available.

The MFWAM model is forced using projected surface wind fields from ARPEGE-Climat (Chauvin et al., 2020), which considers the RCP8.5 future greenhouse gas emission scenario, and include data through 2080. Recently, new Shared Socio-Economic Pathways (SSP) have been developed (Riahi et al., 2017) and adopted within the *IPCC 6<sup>th</sup> Assessment Report (AR6)* together with CMIP6, a new generation of climate models (Eyring et al., 2016). ARPEGE-Climat is developed from one of the CMIP6 models (Roehrig et al., 2020; Voldoire et al., 2013) and has been specifically adapted to properly resolve the atmospheric circulation over the Atlantic basin (Chauvin et al., 2020). However, while ARPEGE-Climat provides state-of-the-art wind projections for our study area, further applications based on SSP scenarios and extending through 2100 would allow coordinating the approach with existing wave projections, such as COWCLIP.

## 5 Conclusions

Five-member ensemble simulations of present-day and future (RCP-8.5) wave climate over the Atlantic Ocean at  $0.5^\circ$  resolution are forced with wind fields from a single high-resolution GCM to investigate winter wave climate change offshore of French Guiana. Despite an expected increase in wind speed over the French Guiana region, the future wave projections revealed a decrease in average and extreme wave heights and periods across winter, mostly associated with weaker swells from the North Atlantic. A slight clockwise rotation of the incident waves is also expected. The consistency between our projected changes and the COWCLIP multi-model predictions for the French Guiana region strengthens the confidence in the wave projections presented here. The

simulated changes in mean winter wave properties are similar to the ones resulting from existing projections for the summer season, and may contribute to changes in coastal morphodynamics for the French Guiana coast, particularly mud bank dynamics. The comparison between modelled wave climate and the available data highlighted the need for the acquisition of long time series of wave conditions offshore of French Guiana, in order to better assess model skill and correct possible systematic model biases.

Our winter wave projections may have significant implications for the prediction of French Guiana's coastal evolution and flood hazard. We highlight the importance of accounting not only for sea-level rise but also for future wave climate change.

## Acknowledgements

This study uses altimeter wave data from the ESA-CCI Sea State Project (<https://climate.esa.int/en/projects/sea-state/>), ERA5 reanalysis wave data produced by the European Centre for Medium-Range Weather Forecasts and distributed by Copernicus (<https://cds.climate.copernicus.eu/cdsapp#!/dataset/reanalysis-era5-single-levels?tab=form>), and CANDHIS wave buoy data (<https://candhis.cerema.fr/public/cartes.php>). The authors thank F. Chauvin for providing the ARPEGE-Climat model results produced within the C3AF (Changement Climatique et Conséquences sur les Antilles Françaises) project; the COWCLIP contributors for providing freely available multi-model global wave projections; G. Le Cozannet for early discussions; and the anonymous reviewers for the comments. MFWAM model data available upon request.

**Funding:** This work was supported by the Direction Générale des Territoires et de la Mer (DGTM), the Agence Française de Développement (AFD), the Agence de l'Environnement et de la Maîtrise de l'Energie (ADEME), the Office de l'Eau de Guyane (OEG), Météo France and BRGM.

## References

- Abascal-Zorrilla, Noelia, Vincent Vantrepotte, Erwan Gensac, Nicolas Huybrechts, and Antoine Gardel. 2018. "The Advantages of Landsat 8-OLI-Derived Suspended Particulate Matter Maps for Monitoring the Subtidal Extension of Amazonian Coastal Mud Banks (French Guiana)." *Remote Sensing* 10(11):1–17. doi: 10.3390/rs10111733.
- Abascal-Zorrilla, Noelia, Vincent Vantrepotte, Nicolas Huybrechts, Dat Dinh Ngoc, Edward J. Anthony, and Antoine Gardel. 2020. "Dynamics of the Estuarine Turbidity Maximum Zone from Landsat-8 Data: The Case of the Maroni River Estuary, French Guiana." *Remote Sensing* 12(13):2173. doi: 10.3390/rs12132173.
- Aertgeerts, Geoffrey, and François Longueville. 2018. *Recensement et Examen Des Aléaslittoraux Guyanais Entre 1993 et 2015*. Cayenne.
- Anthony, E. J., F. Dolique, A. Gardel, and D. Marin. 2011. "Contrasting Sand Beach Morphodynamics in a Mud-Dominated Setting: Cayenne, French Guiana." *Journal of Coastal Research* 30–34. doi: <http://www.jstor.org/stable/26482127>.
- Anthony, Edward J., Antoine Gardel, Nicolas Gratiot, Christophe Proisy, Mead A. Allison, Franck Dolique, and François Fromard. 2010. "The Amazon-Influenced Muddy Coast of South America: A Review of Mud-Bank–Shoreline Interactions." *Earth-Science Reviews* 103(3–4):99–121. doi: 10.1016/j.earscirev.2010.09.008.



- Ardhuin, F. Abrice, E. Rick Rogers, Alexander V Babanin, Jean Francois Filipot, Rudy Magne, Aaron Roland, Andre van der Westhuysen, Pierre Queffeuilou, Jean-Michel Lefevre, Lotfi Aouf, and Fabrice Collard. 2010. “Semiempirical Dissipation Source Functions for Ocean Waves . Part I : Definition , Calibration , and Validation.” *Journal of Physical Oceanography* 40(9):1917–1941. doi: 10.1175/2010JPO4324.1.
- Belmadani, Ali, Alice Dalphinnet, Fabrice Chauvin, Romain Pilon, and Philippe Palany. 2021. “Projected Future Changes in Tropical Cyclone - Related Wave Climate in the North Atlantic.” *Climate Dynamics* 56(11):3687–3708. doi: 10.1007/s00382-021-05664-5.
- Benjamini, Yoav, and Yosef Hochberg. 1995. “Controlling the False Discovery Rate: A Practical and Powerful Approach to Multiple Testing.” *Journal of the Royal Statistical Society: Series B (Methodological)* 57(1):289–300. doi: 10.1111/j.2517-6161.1995.tb02031.x.
- Bernardino, M., M. Gonçalves, and C. Guedes Soares. 2021. “Marine Climate Projections Toward the End of the Twenty-First Century in the North Atlantic.” *Journal of Offshore Mechanics and Arctic Engineering* 143(6). doi: 10.1115/1.4050698.
- Bidlot, J. R. 2017. “Twenty-One Years of Wave Forecast Verification.” *ECMWF Newsletter* 150:31–36.
- Bitner-Gregersen, Elzbieta M., Takuji Waseda, Josko Parunov, Solomon Yim, Spyros Hirdaris, Ning Ma, and C. Guedes Soares. 2022. “Uncertainties in Long-Term Wave Modelling.” *Marine Structures* 84:103217. doi: 10.1016/j.marstruc.2022.103217.
- Bricheno, Lucy M., and Judith Wolf. 2018. “Future Wave Conditions of Europe, in Response to High- End Climate Change Scenarios.” *Journal of Geophysical Research: Oceans* 123(12):8762–91. doi: 10.1029/2018JC013866.
- Camus, P., I. J. Losada, C. Izaguirre, A. Espejo, M. Menéndez, and J. Pérez. 2017. “Statistical Wave Climate Projections for Coastal Impact Assessments.” *Earth’s Future* 5(9):918–33. doi: 10.1002/2017EF000609.
- Cantet, Philippe, Ali Belmadani, Fabrice Chauvin, and Philippe Palany. 2021. “Projections of Tropical Cyclone Rainfall over Land with an Eulerian Approach: Case Study of Three Islands in the West Indies.” *International Journal of Climatology* 41(S1). doi: 10.1002/joc.6760.
- Casas-Prat, M., X. L. Wang, and N. Swart. 2018. “CMIP5-Based Global Wave Climate Projections Including the Entire Arctic Ocean.” *Ocean Modelling* 123(November 2017):66–85. doi: 10.1016/j.ocemod.2017.12.003.
- Casas-Prat, Mercè, Mark A. Hemer, Guillaume Dodet, Joao Morim, Xiaolan L. Wang, Nobuhito Mori, Ian Young, Li Erikson, Bahareh Kamranzad, Prashant Kumar, Melisa Menéndez, and Yang Feng. 2024. “Wind-Wave Climate Changes and Their Impacts.” *Nature Reviews Earth & Environment* 5(1):23–42. doi: 10.1038/s43017-023-00502-0.
- Charles, Elodie, Déborah Idier, Pascale Delecluse, Michel Déqué, and Gonéri Le Cozannet. 2012. “Climate Change Impact on Waves in the Bay of Biscay, France.” *Ocean Dynamics* 62(6). doi: 10.1007/s10236-012-0534-8.
- Chauvin, Fabrice, Romain Pilon, Philippe Palany, and Ali Belmadani. 2020. “Future Changes in Atlantic Hurricanes with the Rotated-Stretched ARPEGE-Climat at Very High Resolution.” *Climate Dynamics* 54(1–2):947–72. doi: 10.1007/s00382-019-05040-4.

- Collins, Jennifer M., and David R. Roache. 2017. “The 2016 North Atlantic Hurricane Season: A Season of Extremes.” *Geophysical Research Letters* 44(10):5071–77. doi: 10.1002/2017GL073390.
- Cooley, S., D. Schoeman, L. Bopp, P. Boyd, S. Donner, S. i. Ito, W. Kiessling, P. Martinetto, E. Ojea, M. F. Racault, B. Rost, M. Skern-Mauritzen, D. Y. Ghebrehiwet, J. D. Bell, J. Blanchard, J. Bolin, W. W. Cheung, A. Cisneros-Montemayor, S. Dupont, S. Dutkiewicz, T. Frölicher, J. D. Gaitán-Espitia, J. G. Molinos, H. Gurney-Smith, S. Henson, M. Hidalgo, E. Holland, R. Kopp, R. Kordas, L. Kwiatkowski, N. Le Bris, S. E. Lluch-Cota, C. Logan, F. C. Mark, Y. Mgaya, C. Moloney, N. P. Muñoz Sevilla, G. Randin, N. B. Raja, A. Rajkaran, A. Richardson, S. Roe, R. Ruiz Diaz, D. Salili, J. B. Sallée, K. Scales, M. Scobie, C. T. Simmons, O. Torres, and A. Yool. 2022. “Oceans and Coastal Ecosystems and Their Services.” in *Climate Change 2022: Impacts, adaptation and vulnerability. Contribution of the WGII to the 6th assessment report of the intergovernmental panel on climate change. IPCC AR6 WGII*, [https://www.ipcc.ch/report/ar6/wg2/downloads/report/IPCC\\_AR6\\_WGII\\_FinalDraft](https://www.ipcc.ch/report/ar6/wg2/downloads/report/IPCC_AR6_WGII_FinalDraft), edited by Cambridge University Press. [https://www.ipcc.ch/report/ar6/wg2/downloads/report/IPCC\\_AR6\\_WGII\\_FinalDraft\\_Chapter03.pdf](https://www.ipcc.ch/report/ar6/wg2/downloads/report/IPCC_AR6_WGII_FinalDraft_Chapter03.pdf).
- Le Cozannet, Gonéri, Déborah Idier, Marcello de Michele, Yoann Legendre, Manuel Moisan, Rodrigo Pedreros, Rémi Thiéblemont, Giorgio Spada, Daniel Raucoules, and Ywenn de la Torre. 2021. “Timescales of Emergence of Chronic Flooding in the Major Economic Center of Guadeloupe.” *Natural Hazards and Earth System Sciences* 21(2):703–22. doi: 10.5194/nhess-21-703-2021.
- D’Agostini, Andressa, Mariana Bernardino, and C. Guedes Soares. 2022. “Projected Wave Storm Conditions under the RCP8.5 Climate Change Scenario in the North Atlantic Ocean.” *Ocean Engineering* 266(P3):112874. doi: 10.1016/j.oceaneng.2022.112874.
- D’Anna, Maurizio, Déborah Idier, Bruno Castelle, Jérémy Rohmer, Laura Cagigal, and Fernando J. Mendez. 2022. “Effects of Stochastic Wave Forcing on Probabilistic Equilibrium Shoreline Response across the 21st Century Including Sea-Level Rise.” *Coastal Engineering* 175(May):104149. doi: 10.1016/j.coastaleng.2022.104149.
- Déqué, Michel. 2007. “Frequency of Precipitation and Temperature Extremes over France in an Anthropogenic Scenario: Model Results and Statistical Correction According to Observed Values.” *Global and Planetary Change* 57:16–26.
- Dodet, Guillaume, Jean-François Piolle, Yves Quilfen, Saleh Abdalla, Mickaël Accensi, Fabrice Ardhuin, Ellis Ash, Jean-Raymond Bidlot, Christine Gommenginger, Gwendal Marechal, Marcello Passaro, Graham Quartly, Justin Stopa, Ben Timmermans, Ian Young, Paolo Cipollini, and Craig Donlon. 2020. “The Sea State CCI Dataset v1: Towards a Sea State Climate Data Record Based on Satellite Observations.” *Earth System Science Data* 12(3):1929–51. doi: 10.5194/essd-12-1929-2020.
- Eisma, D., P. G. E. F. Augustinus, and C. Alexander. 1991. “Recent and Subrecent Changes in the Dispersal of Amazon Mud.” *Netherlands Journal of Sea Research* 28(3):181–92. doi: 10.1016/0077-7579(91)90016-T.
- Erikson, L., J. Morim, M. Hemer, I. Young, X. L. Wang, L. Mentaschi, N. Mori, A. Semedo, J. Stopa, V. Grigorieva, S. Gulev, O. Aarnes, J. R. Bidlot, Ø. Breivik, L. Bricheno, T. Shimura, M. Menendez, M. Markina, V. Sharmar, C. Trenham, J. Wolf, C. Appendini, S. Caires, N. Groll, and A. Webb. 2022. “Global Ocean Wave Fields Show Consistent Regional Trends between 1980 and 2014 in a Multi-Product Ensemble.” *Communications Earth & Environment* 3(1):320. doi: 10.1038/s43247-022-00654-9.

- Eyring, Veronika, Sandrine Bony, Gerald A. Meehl, Catherine A. Senior, Bjorn Stevens, Ronald J. Stouffer, and Karl E. Taylor. 2016. "Overview of the Coupled Model Intercomparison Project Phase 6 (CMIP6) Experimental Design and Organization." *Geoscientific Model Development* 9(5):1937–58. doi: 10.5194/gmd-9-1937-2016.
- Fan, Yalin, Isaac M. Held, Shian-Jiann Lin, and Xiaolan L. Wang. 2013. "Ocean Warming Effect on Surface Gravity Wave Climate Change for the End of the Twenty-First Century." *Journal of Climate* 26(16):6046–66. doi: 10.1175/JCLI-D-12-00410.1.
- Fan, Yalin, Shian-Jiann Lin, Stephen M. Griffies, and Mark A. Hemer. 2014. "Simulated Global Swell and Wind-Sea Climate and Their Responses to Anthropogenic Climate Change at the End of the Twenty-First Century." *Journal of Climate* 27(10):3516–36. doi: 10.1175/JCLI-D-13-00198.1.
- Froidefond, J. M., M. Pujos, and X. Andre. 1988. "Migration of Mud Banks and Changing Coastline in French Guiana." *Marine Geology* 84(1–2):19–30. doi: 10.1016/0025-3227(88)90122-3.
- Gardel, Antoine, and Nicolas Gratiot. 2005. "A Satellite Image-Based Method for Estimating Rates of Mud Bank Migration, French Guiana, South America." *Journal of Coastal Research* 21(4):720–28. doi: 10.2112/03-0100.1.
- Gensac, E., S. Lesourd, A. Gardel, E. J. Anthony, C. Proisy, and H. Loisel. 2011. "Short-Term Prediction of the Evolution of Mangrove Surface Areas: The Example of the Mud Banks of Kourou and Sinnamary, French Guiana." *Journal of Coastal Research* (SPEC. ISSUE 64):388–92.
- Gensac, Erwan, Antoine Gardel, Sandric Lesourd, and Laurent Brutier. 2015. "Morphodynamic Evolution of an Intertidal Mudflat under the Influence of Amazon Sediment Supply – Kourou Mud Bank, French Guiana, South America." *Estuarine, Coastal and Shelf Science* 158:53–62. doi: 10.1016/j.ecss.2015.03.017.
- Gratiot, Nicolas, Antoine Gardel, and Edward J. Anthony. 2007. "Trade-Wind Waves and Mud Dynamics on the French Guiana Coast, South America: Input from ERA-40 Wave Data and Field Investigations." *Marine Geology* 236(1–2):15–26. doi: 10.1016/j.margeo.2006.09.013.
- Hawkins, Timothy W., Isabelle Gouirand, Theodore Allen, and Ali Belmadani. 2022. "Atmospheric Drivers of Oceanic North Swells in the Eastern Caribbean." *Journal of Marine Science and Engineering* 10(2):183. doi: 10.3390/jmse10020183.
- Hemer, Mark A., Yalin Fan, Nobuhito Mori, Alvaro Semedo, and Xiaolan L. Wang. 2013. "Projected Changes in Wave Climate from a Multi-Model Ensemble." *Nature Climate Change* 3(5):471–76. doi: 10.1038/nclimate1791.
- Hemer, Mark A., Jack Katzfey, and Claire E. Trenham. 2013. "Global Dynamical Projections of Surface Ocean Wave Climate for a Future High Greenhouse Gas Emission Scenario." *Ocean Modelling* 70:221–45. doi: 10.1016/j.ocemod.2012.09.008.
- Hemer, Mark A., X. Wang, A. Webb, and COWCLIP. 2018. *Report of the 2018 Meeting for the WCRP-JCOMM Coordinated Global Wave Climate Projections.*
- Hersbach, Hans, Bill Bell, Paul Berrisford, Shoji Hirahara, András Horányi, Joaquín Muñoz- Sabater, Julien Nicolas, Carole Peubey, Raluca Radu, Dinand Schepers, Adrian Simmons, Cornel Soci, Saleh Abdalla, Xavier Abellan, Gianpaolo Balsamo, Peter Bechtold, Gionata Biavati, Jean Bidlot, Massimo Bonavita, Giovanna Chiara, Per Dahlgren, Dick Dee, Michail Diamantakis, Rossana Dragani, Johannes Flemming, Richard Forbes, Manuel Fuentes, Alan Geer, Leo Haimberger, Sean Healy, Robin J. Hogan, Elías Hólm, Marta Janisková, Sarah Keeley, Patrick Laloyaux, Philippe Lopez, Cristina Lupu, Gabor Radnoti, Patricia Rosnay, Iryna Rozum, Freja

- Vamborg, Sebastien Villaume, and Jean- Noël Thépaut. 2020. “The ERA5 Global Reanalysis.” *Quarterly Journal of the Royal Meteorological Society* 146(730):1999–2049. doi: 10.1002/qj.3803.
- Hinkel, J., L. Feyen, Mark A. Hemer, G. Le Cozannet, D. Lincke, M. Marcos, L. Mentaschi, J. L. Merkens, H. de Moel, S. Muis, R. J. Nicholls, A. T. Vafeidis, R. S. W. van de Wal, M. I. Vousdoukas, T. Wahl, P. J. Ward, and C. Wolff. 2021. “Uncertainty and Bias in Global to Regional Scale Assessments of Current and Future Coastal Flood Risk.” *Earth’s Future* 9(7). doi: 10.1029/2020EF001882.
- Hinkel, Jochen, John A. Church, Jonathan M. Gregory, Erwin Lambert, Gonéri Le Cozannet, Jason Lowe, Kathleen L. McInnes, Robert J. Nicholls, Thomas D. Pol, and Roderik Wal. 2019. “Meeting User Needs for Sea Level Rise Information: A Decision Analysis Perspective.” *Earth’s Future* 7(3):320–37. doi: 10.1029/2018EF001071.
- Jolivet, Morgane, Edward J. Anthony, Antoine Gardel, Tanguy Maury, and Sylvain Morvan. 2022. “Dynamics of Mud Banks and Sandy Urban Beaches in French Guiana, South America.” *Regional Environmental Change* 22(3):101. doi: 10.1007/s10113-022-01944-w.
- Jolivet, Morgane, Antoine Gardel, and Edward J. Anthony. 2019. “Multi-Decadal Changes on the Mud-Dominated Coast of Western French Guiana: Implications for Mesoscale Shoreline Mobility, River-Mouth Deflection, and Sediment Sorting.” *Journal of Coastal Research* 88(sp1):185. doi: 10.2112/SI88-014.1.
- Khandekar, M. L. 1989. “Validation of Wave Models.” Pp. 127–64 in *Operational Analysis and Prediction of Ocean Wind Waves*. New York, NY: Springer New York.
- Kodaira, Tsubasa, Kaushik Sasmal, Rei Miratsu, Tsutomu Fukui, Tingyao Zhu, and Takuji Waseda. 2023. “Uncertainty in Wave Hindcasts in the North Atlantic Ocean.” *Marine Structures* 89:103370. doi: 10.1016/j.marstruc.2023.103370.
- Lakhan, V. Chris, and David A. Pepper. 1997. “Relationship between Concavity and Convexity of a Coast and Erosion and Accretion Patterns.” *Journal of Coastal Research* 13(1):226–32. doi: <https://www.jstor.org/stable/4298609>.
- Lemos, Gil, Ivana Bosnic, Carlos Antunes, Michalis Vousdoukas, Lorenzo Mentaschi, Miguel Espírito Santo, Vanessa Ferreira, and Pedro M. M. Soares. 2024. “The Future of the Portuguese (SW Europe) Most Vulnerable Coastal Areas under Climate Change – Part II: Future Extreme Coastal Flooding from Downscaled Bias Corrected Wave Climate Projections.” *Ocean Engineering* 310:118448. doi: 10.1016/j.oceaneng.2024.118448.
- Lemos, Gil, Melisa Menendez, Alvaro Semedo, Paula Camus, Mark A. Hemer, Mikhail Dobrynin, and Pedro M. A. Miranda. 2020. “On the Need of Bias Correction Methods for Wave Climate Projections.” *Global and Planetary Change* 186:103109. doi: 10.1016/j.gloplacha.2019.103109.
- Lemos, Gil, Melisa Menendez, Alvaro Semedo, Pedro M. A. Miranda, and Mark A. Hemer. 2021. “On the Decreases in North Atlantic Significant Wave Heights from Climate Projections.” *Climate Dynamics* 57(9):2301–24. doi: 10.1007/s00382-021-05807-8.
- Lemos, Gil, Alvaro Semedo, Mikhail Dobrynin, Arno Behrens, Joanna Staneva, Jean-Raymond Bidlot, and Pedro M. A. Miranda. 2019. “Mid-Twenty-First Century Global Wave Climate Projections: Results from a Dynamic CMIP5 Based Ensemble.” *Global and Planetary Change* 172:69–87. doi: <https://doi.org/10.1016/j.gloplacha.2018.09.011>.

- Lira Loarca, Andrea, Peter Berg, Asuncion Baquerizo, and Giovanni Besio. 2023. “On the Role of Wave Climate Temporal Variability in Bias Correction of Wave Climate Projections.” *Climate Dynamics*. doi: <https://doi.org/10.21203/rs.3.rs-1986616/v1>.
- Lobeto, Hector, Melisa Menendez, and Iñigo J. Losada. 2021. “Future Behavior of Wind Wave Extremes Due to Climate Change.” *Scientific Reports* 11(1):7869. doi: 10.1038/s41598-021-86524-4.
- Lobeto, Hector, Melisa Menendez, Iñigo J. Losada, and Mark A. Hemer. 2022. “The Effect of Climate Change on Wind-Wave Directional Spectra.” *Global and Planetary Change* 213:103820. doi: 10.1016/j.gloplacha.2022.103820.
- Longueville, François. 2017. *Rapport d'expertise: Observations Suite Aux Épisodes d'érosion Marine de Fin d'année 2016 Sur Le Littoral de Kourou (Guyane)*. Cayenne.
- Longueville, François, and Méline Lanson. 2022. *Épisodes d'érosion Du 3 Au 7 Janvier 2022 Sur Le Littoral d'Awala-Yalimapo (Guyane) : Avis et Recommandations Du BRGM*. Cayenne.
- Longueville, François, Rémi Thiéblemont, Ali Belmadani, Déborah Idier, Philippe Palany, Maurizio D'Anna, Pierre-Christian Dutrieux, Léopold Védie, Méline Lanson, and Baptiste Suez-Panama-Bouton. 2022. *Impacts Du Changement Climatique Sur Différents Paramètres Physiques En Guyane : Caractérisation et Projection - GuyaClimat*.
- Mankin, Justin S., Flavio Lehner, Sloan Coats, and Karen A. McKinnon. 2020. “The Value of Initial Condition Large Ensembles to Robust Adaptation Decision- Making.” *Earth's Future* 8(10). doi: 10.1029/2020EF001610.
- Meucci, Alberto, Ian R. Young, Mark A. Hemer, Ebru Kirezci, and Roshanka Ranasinghe. 2020. “Projected 21st Century Changes in Extreme Wind-Wave Events.” *Science Advances* 6(24). doi: 10.1126/sciadv.aaz7295.
- Meucci, Alberto, Ian R. Young, Mark Hemer, Claire Trenham, and Ian G. Watterson. 2023. “140 Years of Global Ocean Wind-Wave Climate Derived from CMIP6 ACCESS-CM2 and EC-Earth3 GCMs: Global Trends, Regional Changes, and Future Projections.” *Journal of Climate* 36(6):1605–31. doi: 10.1175/JCLI-D-21-0929.1.
- Meucci, Alberto, Ian R. Young, Claire Trenham, and Mark Hemer. 2024. “An 8-Model Ensemble of CMIP6-Derived Ocean Surface Wave Climate.” *Scientific Data* 11(1):100. doi: 10.1038/s41597-024-02932-x.
- Mori, Nobuhito, Tomoya Shimura, Tomohiro Yasuda, and Hajime Mase. 2013. “Multi-Model Climate Projections of Ocean Surface Variables under Different Climate Scenarios—Future Change of Waves, Sea Level and Wind.” *Ocean Engineering* 71:122–29. doi: 10.1016/j.oceaneng.2013.02.016.
- Mori, Nobuhito, Tomohiro Yasuda, Hajime Mase, Tracey Tom, and Yuichiro Oku. 2010. “Projection of Extreme Wave Climate Change under Global Warming.” 19:15–19. doi: 10.3178/HRL.4.15.
- Morim, J., L. H. Erikson, M. Hemer, I. Young, X. Wang, N. Mori, T. Shimura, J. Stopa, C. Trenham, L. Mentaschi, S. Gulev, V. D. Sharmar, L. Bricheno, J. Wolf, O. Aarnes, J. Perez, J. Bidlot, A. Semedo, B. Reguero, and T. Wahl. 2022. “A Global Ensemble of Ocean Wave Climate Statistics from Contemporary Wave Reanalysis and Hindcasts.” *Scientific Data* 9(1):358. doi: 10.1038/s41597-022-01459-3.
- Morim, Joao, Mark Hemer, Xiaolan L. Wang, Nick Cartwright, Claire Trenham, Alvaro Semedo, Ian Young, Lucy Bricheno, Paula Camus, Mercè Casas-Prat, Li Erikson, Lorenzo Mentaschi,

- Nobuhito Mori, Tomoya Shimura, Ben Timmermans, Ole Aarnes, Øyvind Breivik, Arno Behrens, Mikhail Dobrynin, Melisa Menendez, Joanna Staneva, Michael Wehner, Judith Wolf, Bahareh Kamranzad, Adrean Webb, Justin Stopa, and Fernando Andutta. 2019. “Robustness and Uncertainties in Global Multivariate Wind-Wave Climate Projections.” *Nature Climate Change* 9(9). doi: 10.1038/s41558-019-0542-5.
- Morim, Joao, Claire Trenham, Mark Hemer, Xiaolan L. Wang, Nobuhito Mori, Mercè Casas-Prat, Alvaro Semedo, Tomoya Shimura, Ben Timmermans, Paula Camus, Lucy Bricheno, Lorenzo Mentaschi, Mikhail Dobrynin, Yang Feng, and Li Erikson. 2020. “A Global Ensemble of Ocean Wave Climate Projections from CMIP5-Driven Models.” *Scientific Data* 7(1):105. doi: 10.1038/s41597-020-0446-2.
- Morim, Joao, Thomas Wahl, Sean Vitousek, Sara Santamaria-Aguilar, Ian R. Young, and Mark A. Hemer. 2023. “Understanding Uncertainties in Contemporary and Future Extreme Wave Events for Broad-Scale Impact and Adaptation Planning.” *Science Advances* 9(2). doi: 10.1126/sciadv.ade3170.
- Parodi, Matteo U., Alessio Giardino, Ap van Dongeren, Stuart G. Pearson, Jeremy D. Bricker, and Ad J. H. M. Reniers. 2020. “Uncertainties in Coastal Flood Risk Assessments in Small Island Developing States.” *Natural Hazards and Earth System Sciences* 20(9):2397–2414. doi: 10.5194/nhess-20-2397-2020.
- Piollé, J. F., G. Dodet, Y. Quilfen, and ESA Sea State Climate Change Initiative. 2020. *Global Remote Sensing Merged Multi-Mission Monthly Gridded Significant Wave Height, L4 Product, Version 1.1*.
- Rayner, N. A. 2003. “Global Analyses of Sea Surface Temperature, Sea Ice, and Night Marine Air Temperature since the Late Nineteenth Century.” *Journal of Geophysical Research* 108(D14):4407. doi: 10.1029/2002JD002670.
- Reguero, Borja G., Iñigo J. Losada, and Fernando J. Méndez. 2019. “A Recent Increase in Global Wave Power as a Consequence of Oceanic Warming.” *Nature Communications* 10(1):205. doi: 10.1038/s41467-018-08066-0.
- Riahi, Keywan, Detlef P. van Vuuren, Elmar Kriegler, Jae Edmonds, Brian C. O’Neill, Shinichiro Fujimori, Nico Bauer, Katherine Calvin, Rob Dellink, Oliver Fricko, Wolfgang Lutz, Alexander Popp, Jesus Crespo Cuaresma, Samir KC, Marian Leimbach, Leiwen Jiang, Tom Kram, Shilpa Rao, Johannes Emmerling, Kristie Ebi, Tomoko Hasegawa, Petr Havlik, Florian Humpenöder, Lara Aleluia Da Silva, Steve Smith, Elke Stehfest, Valentina Bosetti, Jiyong Eom, David Gernaat, Toshihiko Masui, Joeri Rogelj, Jessica Strefler, Laurent Drouet, Volker Krey, Gunnar Luderer, Mathijs Harmsen, Kiyoshi Takahashi, Lavinia Baumstark, Jonathan C. Doelman, Mikiko Kainuma, Zbigniew Klimont, Giacomo Marangoni, Hermann Lotze-Campen, Michael Obersteiner, Andrzej Tabeau, and Massimo Tavoni. 2017. “The Shared Socioeconomic Pathways and Their Energy, Land Use, and Greenhouse Gas Emissions Implications: An Overview.” *Global Environmental Change* 42:153–68. doi: 10.1016/j.gloenvcha.2016.05.009.
- Roehrig, Romain, Isabelle Beau, David Saint- Martin, Antoinette Alias, Bertrand Decharme, Jean-François Guérémy, Aurore Voldoire, Ahmat Younous Abdel- Lathif, Eric Bazile, Sophie Belamari, Sebastien Blein, Dominique Bouniol, Yves Bouteloup, Julien Cattiaux, Fabrice Chauvin, Matthieu Chevallier, Jeanne Colin, Hervé Douville, Pascal Marquet, Martine Michou, Pierre Nabat, Thomas Oudar, Philippe Peyrillé, Jean- Marcel Piriou, David Salas y Mélia, Roland Sférian, and Stéphane Sénési. 2020. “The CNRM Global Atmosphere Model ARPEGE- Climat 6.3: Description and Evaluation.” *Journal of Advances in Modeling Earth Systems* 12(7). doi: 10.1029/2020MS002075.

- Semedo, Alvaro, Mikhail Dobrynin, Gil Lemos, Arno Behrens, Joanna Staneva, Hylke de Vries, Andreas Sterl, Jean-Raymond Bidlot, Pedro Miranda, and Jens Murawski. 2018. "CMIP5-Derived Single-Forcing, Single-Model, and Single-Scenario Wind-Wave Climate Ensemble: Configuration and Performance Evaluation." *Journal of Marine Science and Engineering* 6(3):90. doi: 10.3390/jmse6030090.
- Semedo, Alvaro, Ralf Weisse, Arno Behrens, Andreas Sterl, Lennart Bengtsson, and Heinz Gunther. 2013. "Projection of Global Wave Climate Change toward the End of the Twenty-First Century." *Journal of Climate* 26(21):8269–88. doi: 10.1175/JCLI-D-12-00658.1.
- Semedo, Alvaro, Ralf Weisse, Arno Behrens, Andreas Sterl, Lennart Bengtsson, and Heinz Günther. 2012. "Projection of Global Wave Climate Change toward the End of the Twenty-First Century." *Journal of Climate* 26(21):8269–88. doi: 10.1175/JCLI-D-12-00658.1.
- Timmermans, Ben, C. P. Gommenginger, G. Dodet, and J. - R. Bidlot. 2020. "Global Wave Height Trends and Variability from New Multimission Satellite Altimeter Products, Reanalyses, and Wave Buoys." *Geophysical Research Letters* 47(9). doi: 10.1029/2019GL086880.
- Timmermans, Ben, Dáithí Stone, Michael Wehner, and Harinarayan Krishnan. 2017. "Impact of Tropical Cyclones on Modeled Extreme Wind- wave Climate." *Geophysical Research Letters* 44(3):1393–1401. doi: 10.1002/2016GL071681.
- Toimil, Alexandra, Paula Camus, Iñigo J. Losada, and Moises Alvarez-Cuesta. 2021. "Visualising the Uncertainty Cascade in Multi-Ensemble Probabilistic Coastal Erosion Projections." *Frontiers in Marine Science* 8. doi: 10.3389/fmars.2021.683535.
- Toimil, Alexandra, Paula Camus, Iñigo J. Losada, Gonéri Le Cozannet, Robert J. Nicholls, Déborah Idier, and Aurelie Maspataud. 2020. "Climate Change-Driven Coastal Erosion Modelling in Temperate Sandy Beaches: Methods and Uncertainty Treatment." *Earth-Science Reviews* 202. doi: 10.1016/j.earscirev.2020.103110.
- Vantrepotte, V., E. Gensac, H. Loisel, A. Gardel, D. Dessailly, and X. Mériaux. 2013. "Satellite Assessment of the Coupling between in Water Suspended Particulate Matter and Mud Banks Dynamics over the French Guiana Coastal Domain." *Journal of South American Earth Sciences* 44:25–34. doi: 10.1016/j.jsames.2012.11.008.
- Voltaire, A., D. Saint- Martin, S. Sénési, B. Decharme, A. Alias, M. Chevallier, J. Colin, J. - F. Guérémy, M. Michou, M. - P. Moine, P. Nabat, R. Roehrig, D. Salas y Mélia, R. Sférian, S. Valcke, I. Beau, S. Belamari, S. Berthet, C. Cassou, J. Cattiaux, J. Deshayes, H. Douville, C. Ethé, L. Franchistéguy, O. Geoffroy, C. Lévy, G. Madec, Y. Meurdesoif, R. Msadek, A. Ribes, E. Sanchez- Gomez, L. Terray, and R. Waldman. 2019. "Evaluation of CMIP6 DECK Experiments With CNRM- CM6- 1." *Journal of Advances in Modeling Earth Systems* 11(7):2177–2213. doi: 10.1029/2019MS001683.
- Voltaire, A., E. Sanchez-Gomez, D. Salas y Mélia, B. Decharme, C. Cassou, S. Sénési, S. Valcke, I. Beau, A. Alias, M. Chevallier, M. Déqué, J. Deshayes, H. Douville, E. Fernandez, G. Madec, E. Maisonnave, M. P. Moine, S. Planton, D. Saint-Martin, S. Szopa, S. Tyteca, R. Alkama, S. Belamari, A. Braun, L. Coquart, and F. Chauvin. 2013. "The CNRM-CM5.1 Global Climate Model: Description and Basic Evaluation." *Climate Dynamics* 40(9–10):2091–2121. doi: 10.1007/s00382-011-1259-y.
- Vousdoukas, Michalis I., Dimitrios Bouziotas, Alessio Giardino, Laurens M. Bouwer, Lorenzo Mentaschi, Evangelos Voukouvalas, and Luc Feyen. 2018. "Understanding Epistemic Uncertainty in Large-Scale Coastal Flood Risk Assessment for Present and Future Climates." *Natural Hazards and Earth System Sciences* 18(8):2127–42. doi: 10.5194/nhess-18-2127-2018.

- WAMDI-Group. 1988. “The WAM Model: A Third-Generation Ocean Wave Prediction Model.” *Journal of Physical Oceanography* 18:1775–1810.
- Wang, Xiaolan L., Yang Feng, and Val R. Swail. 2014. “Changes in Global Ocean Wave Heights as Projected Using Multimodel CMIP5 Simulations.” *Geophysical Research Letters* 41(3):1026–34. doi: 10.1002/2013GL058650.
- Webb, Adrean, Tomoya Shimura, and Nobuhito Mori. 2018. “A High-Resolution Future Wave Climate Projection for the Coastal Northwestern Atlantic.” *Journal of Japan Society of Civil Engineers, Ser. B2 (Coastal Engineering)* 74(2):1345–50. doi: 10.2208/kaigan.74.I\_1345.
- Wells, John T., and G. Paul Kemp. 1986. “Interaction of Surface Waves and Cohesive Sediments: Field Observations and Geologic Significance.” Pp. 43–65 in *Lecture Notes on Coastal and Estuarine Studies*, edited by A. J. Mehta.
- Yadav, Anshu, Prashant Kumar, Prasad Kumar Bhaskaran, Yukiharu Hisaki, and Rajni. 2024. “Evaluation of Ocean Wave Power Utilizing COWCLIP 2.0 Datasets: A CMIP5 Model Assessment.” *Climate Dynamics*. doi: 10.1007/s00382-024-07402-z.
- Young, Ian R. 1999. “Seasonal Variability of the Global Ocean Wind and Wave Climate.” *International Journal of Climatology* 19:931–50. doi: [https://doi.org/10.1002/\(SICI\)1097-0088\(199907\)](https://doi.org/10.1002/(SICI)1097-0088(199907)19:931-50).

## Author contributions

### *CRedit* author statement

**Maurizio D’Anna:** Conceptualization; Formal Analysis; Investigation; Writing - original draft;

**Léopold Védie:** Formal Analysis, Investigation, Software, Visualization;

**Ali Belmadani:** Conceptualization; Formal Analysis; Methodology; Supervision; Writing-review & editing;

**Déborah Idier:** Conceptualization; Writing- review & editing;

**Rémi Thiéblemont:** Formal Analysis; Writing- review & editing;

**Philippe Palany:** Funding acquisition; Project administration;

**François Longueville:** Funding acquisition; Project administration; Writing- review & editing.



**Declaration of interests**

The authors declare that they have no known competing financial interests or personal relationships that could have appeared to influence the work reported in this paper.

The authors declare the following financial interests/personal relationships which may be considered as potential competing interests:

F. Longueville, P. Palany reports financial support was provided by Direction Générale des Territoires et de la Mer. F. Longueville, P. Palany reports financial support was provided by Agence Française de Développement. F. Longueville, P. Palany reports financial support was provided by Agence de l'Environnement et de la Maîtrise de l'Energie. F. Longueville, P. Palany reports financial support was provided by Office de l'Eau de Guyane. If there are other authors, they declare that they have no known competing financial interests or personal relationships that could have appeared to influence the work reported in this paper.

Journal Pre-proof